MATHEMATICS OF COMPUTATION
Volume 92, Number 341, May 2023, Pages 1109–1139
https://doi.org/10.1090/mcom/3801
Article electronically published on November 29, 2022

IMPROVED UNIFORM ERROR BOUNDS OF THE TIME-SPLITTING METHODS FOR THE LONG-TIME (NONLINEAR) SCHRÖDINGER EQUATION

WEIZHU BAO, YONGYONG CAI, AND YUE FENG

Abstract. We establish improved uniform error bounds for the time-splitting methods for the long-time dynamics of the Schrödinger equation with small potential and the nonlinear Schrödinger equation (NLSE) with weak nonlinearity. For the Schrödinger equation with small potential characterized by a dimensionless parameter $\varepsilon \in (0, 1]$, we employ the unitary flow property of the (second-order) time-splitting Fourier pseudospectral (TSFP) method in L^2-norm to prove a uniform error bound at time $t_\varepsilon = t/\varepsilon$ as $C(t)\widetilde{C}(T)(h^m + \tau^2)$ up to $t_\varepsilon \leq T_\varepsilon = T/\varepsilon$ for any $T > 0$ and uniformly for $\varepsilon \in (0, 1]$, while h is the mesh size, τ is the time step, $m \geq 2$ and $\tilde{C}(T)$ (the local error bound) depend on the regularity of the exact solution, and $C(t) = C_0 + C_1 t$ grows at most linearly with respect to t with C_0 and C_1 two positive constants independent of T, ε, h and τ. Then by introducing a new technique of *regularity compensation oscillation* (RCO) in which the high frequency modes are controlled by regularity and the low frequency modes are analyzed by phase cancellation and energy method, an improved uniform (w.r.t ε) error bound at $O(h^{m-1} + \varepsilon\tau^2)$ is established in H^1-norm for the long-time dynamics up to the time at $O(1/\varepsilon)$ of the Schrödinger equation with $O(\varepsilon)$-potential with $m \geq 3$. Moreover, the RCO technique is extended to prove an improved uniform error bound at $O(h^{m-1} + \varepsilon^2\tau^2)$ in H^1-norm for the long-time dynamics up to the time at $O(1/\varepsilon^2)$ of the cubic NLSE with $O(\varepsilon^2)$-nonlinearity strength. Extensions to the first-order and fourth-order time-splitting methods are discussed. Numerical results are reported to validate our error estimates and to demonstrate that they are sharp.

1. Introduction

The (nonlinear) Schrödinger equation arises in various physical phenomena, such as quantum mechanics, Bose-Einstein condensates, laser beam propagation, plasma and particle physics [2, 20, 31, 32, 47]. In this paper, we consider the following Schrödinger equation

$$i\partial_t \psi(\mathbf{x}, t) = -\Delta\psi(\mathbf{x}, t) + \varepsilon V(\mathbf{x})\psi(\mathbf{x}, t), \ \mathbf{x} \in \Omega, \ t > 0, \tag{1.1}$$

Received by the editor November 10, 2021, and, in revised form, July 3, 2022, and October 12, 2022.

2020 *Mathematics Subject Classification.* Primary 35Q41,35Q55, 65M15, 65M70.

Key words and phrases. Schrödinger equation, nonlinear Schrödinger equation, long-time dynamics, time-splitting Fourier pseudospectal method, improved uniform error bound, regularity compensation oscillation (RCO).

The work of the first and third authors was partially supported by the Ministry of Education of Singapore grant MOE2019-T2-1-063 (R-146-000-296-112) and the work of the second author was supported by Natural Science Foundation of China grant NSFC grant 12171041 and 11771036.

and the nonlinear Schrödinger equation (NLSE)

$$i\partial_t \psi(\mathbf{x},t) = -\Delta\psi(\mathbf{x},t) \pm \varepsilon^2 |\psi(\mathbf{x},t)|^2 \psi(\mathbf{x},t), \ \mathbf{x}\in\Omega, \ t>0, \tag{1.2}$$

with the initial data

$$\psi(\mathbf{x},0) = \psi_0(\mathbf{x}), \quad \mathbf{x}\in\overline{\Omega}, \tag{1.3}$$

where $\Omega = \prod_{i=1}^{d}(a_i,b_i) \subset \mathbb{R}^d$ $(d=1,2,3)$ is a bounded domain equipped with periodic boundary conditions. Here, t is time, $\mathbf{x} = (x_1,\cdots,x_d)^T \in \mathbb{R}^d$ is the spatial coordinate, $\psi(\mathbf{x},t) \in \mathbb{C}$ is the complex order parameter/wave function, $V(\mathbf{x}) \in \mathbb{R}$ is a given external potential, $\varepsilon \in (0,1]$ is a dimensionless parameter. In the Schrödinger equation (1.1), the amplitude of the potential is characterized by the parameter $\varepsilon \in (0,1]$. In the NLSE (1.2), the strength of the nonlinearity is $O(\varepsilon^2)$ – *NLSE with weak nonlinearity* – and the dynamics of the NLSE (1.2) with $O(1)$-initial data is equivalent to the NLSE with $O(1)$-nonlinearity and $O(\varepsilon)$-initial data – *NLSE with small initial data*, e.g. by setting $\phi(\mathbf{x},t) = \varepsilon\psi(\mathbf{x},t)$, the NLSE (1.2) with (1.3) becomes

$$\begin{cases} i\partial_t \phi(\mathbf{x},t) = -\Delta\phi(\mathbf{x},t) \pm |\phi(\mathbf{x},t)|^2 \phi(\mathbf{x},t), \ \mathbf{x}\in\Omega, \ t>0, \\ \phi(\mathbf{x},0) = \varepsilon\psi_0(\mathbf{x}) := \phi_0(\mathbf{x}) = O(\varepsilon), \quad \mathbf{x}\in\overline{\Omega}. \end{cases} \tag{1.4}$$

In the past two decades, many accurate and efficient numerical methods have been proposed and analyzed to simulate the (nonlinear) Schrödinger equation including the finite difference time domain (FDTD) methods [1, 3, 28], the exponential wave integrator Fourier pseudospectral (EWI-FP) method [21, 27, 40], the time-splitting Fourier pseudospectral (TSFP) method [13, 18, 42, 52], etc. Among these numerical methods, the TSFP method preserves a set of geometric properties and performs much better than the other numerical approaches regarding the stability, efficiency, accuracy and spatial/temporal resolution [2, 10, 11]. However, convergence analysis for the TSFP method applied to the (nonlinear) Schrödinger equation is normally valid up to the finite-time dynamics at $O(1)$ and we refer to [10, 13, 32, 38, 42, 50] and references therein.

Recently, long-time behaviors of the (nonlinear) Schrödinger equation on compact domains have received a great deal of attention [16, 19, 30, 32–34]. Along the analytical front, the existence of the solution, the asymptotic behavior and conservation laws have been well studied in the literature [14, 17, 26, 39, 48]. From the viewpoint of numerical analysis, the stability of the plane wave solutions and long-time preservations of the actions and energy for the TSFP method have been shown for the NLSE with the help of Birkhoff normal form and the modulated Fourier expansion [25, 33, 35–37]. For the long-time error estimates of the numerical schemes, improved error bounds for time-splitting methods have been proven under the constraint that the time step τ is an integer fraction of the period of the principal linear part [22]. Due to the usage of the properties for the periodic function, extensions of the improved error bounds to higher dimensions require that the aspect ratio of the domain is rational. In addition, error estimates of the splitting methods have been established with the error bound growing linearly in time for the Maxwell's equations [23, 24] and the Schrödinger equations [41] (semi-discrete-in-time case). However, such linear growth of the fully discrete TSFP error bound for the Schrödinger equation has not been reported.

The aim of this work is to establish the improved uniform error bounds for the TSFP method for the long-time dynamics of the Schrödinger equation with small

potential and the NLSE with weak nonlinearity, removing the previous assumptions on the periodicity of the free Schrödinger evolutionary operator and the integer fraction time steps. First, we prove a uniform error bound in L^2-norm for the TSFP method applied to the Schödinger equation with the constant in the error bound growing linearly with respect to the time t. Based on this error bound, for a given accuracy tolerance δ_0 and time step τ, we could obtain the computational time within the accuracy δ_0 by using the TSFP method is $O(\delta_0/\tau^2)$ for $\varepsilon = 1$, i.e., with the smaller time step τ, the longer dynamics for the Schrödinger equation can be calculated! Then by introducing a new technique of **regularity compensation oscillation** (RCO) in which the high frequency modes are controlled by regularity and the low frequency modes are analyzed by phase cancellation and energy method, an improved uniform error bound in H^1-norm for the Schrödinger equation with $O(\varepsilon)$-potential up to the time $O(1/\varepsilon)$ is carried out at $O(h^{m-1} + \varepsilon\tau^2 + \tau_0^{m-1})$ with $m \geq 3$ depending on the regularity of the exact solution and $\tau_0 \in (0, 1)$ a parameter fixed. In addition, the technique of RCO is extended to the proof of an improved uniform error bound for the cubic NLSE with $O(\varepsilon^2)$-nonlinearity strength up to the time at $O(1/\varepsilon^2)$ with the error bound in H^1-norm at $O(h^{m-1} + \varepsilon^2\tau^2 + \tau_0^{m-1})$.

Here, we briefly explain the idea of our analysis. For sufficiently regular solution, we use the smoothness of the exact solution to control the high frequency modes ($> 1/\tau_0$) as τ_0^{m-1}, where τ_0 is a chosen frequency cut-off parameter. The low frequency modes ($\leq 1/\tau_0$) will be treated by the RCO technique for sufficiently small τ and non-resonant τ, which basically asserts that the error of the low frequency part behaves much better (satisfies the improved error bounds) as long as the time step size τ is non-resonant or resolves the frequency. The regularity compensation oscillation (RCO) comes from the facts that the high modes are bounded by the regularity of the exact solution and an order of ε could be gained by noticing that $i\partial_t\psi + \Delta\psi = O(\varepsilon\psi)$ from (1.1), and respectively, an order of ε^2 could be gained by $i\partial_t\psi + \Delta\psi = O(\varepsilon^2|\psi|^2\psi)$ from (1.2), i.e., a suitable combination of higher order derivatives could compensate the wave oscillation of magnitude $O(\varepsilon)/O(\varepsilon^2)$.

The rest of this paper is organized as follows. In Section 2, the uniform error bound for the TSFP method in L^2-norm for the Schrödinger equation with $O(\varepsilon)$-potential up to the final time $T_\varepsilon = T/\varepsilon$ is proven and the error is shown to grow linearly with respect to T. Then, the improved uniform error bound in H^1-norm is rigorously established with the help of a new technique of regularity compensation oscillation (RCO). In Section 3, the RCO technique is extended to analyze the improved uniform error bound in H^1-norm for the cubic NLSE with $O(\varepsilon^2)$-nonlinearity strength up to the final long-time at $O(1/\varepsilon^2)$. In Sections 2 and 3, extensive numerical results are reported to validate our error estimates and demonstrate that they are sharp. Finally, some conclusions are drawn in Section 4. Throughout the paper, the notation $A \lesssim B$ is used to represent that there exists a generic constant $C > 0$, which is independent of the mesh size h, time step τ and ε such that $|A| \leq CB$.

2. Improved uniform error bounds for the Schrödinger equation

In this section, we adopt the time-splitting Fourier pseudospectral (TSFP) method to numerically solve the Schrödinger equation (1.1) and rigorously establish the uniform error bound in L^2-norm and improved uniform error bound in H^1-norm using RCO. For the simplicity of presentation, we only carry out the analysis in

one dimension (1D) and generalizations to higher dimensions are straightforward (see also Remark 2.9 for discussion). In 1D, the Schrödinger equation (1.1) with the initial data (1.3) and periodic boundary conditions on the domain $\Omega = (a, b)$ can be written as

$$\begin{cases} i\partial_t \psi(x,t) = -\Delta\psi(x,t) + \varepsilon V(x)\psi(x,t), & a < x < b,\ t > 0, \\ \psi(a,t) = \psi(b,t),\ \partial_x\psi(a,t) = \partial_x\psi(b,t), & t \geq 0, \\ \psi(x,0) = \psi_0(x), & x \in [a,b]. \end{cases} \tag{2.1}$$

2.1. **The TSFP method.** By the splitting technique [42, 43, 49], the Schrödinger equation (2.1) can be decomposed into two subproblems. The first one is

$$\begin{cases} i\partial_t \psi(x,t) = -\Delta\psi(x,t), & x \in \Omega, \quad t > 0, \\ \psi(a,t) = \psi(b,t),\ \partial_x\psi(a,t) = \partial_x\psi(b,t), & t \geq 0, \\ \psi(x,0) = \psi_0(x),\ x \in [a,b], \end{cases} \tag{2.2}$$

which can be solved exactly in phase space

$$\psi(\cdot,t) = e^{it\Delta}\psi_0(\cdot), \quad t \geq 0. \tag{2.3}$$

The second one is to solve

$$\begin{cases} i\partial_t \psi(x,t) = \varepsilon V(x)\psi(x,t), & x \in \Omega, \quad t > 0, \\ \psi(x,0) = \psi_0(x), & x \in [a,b], \end{cases} \tag{2.4}$$

which can be integrated exactly in time, for $x \in [a, b]$, as

$$\psi(x,t) = e^{-i\varepsilon t V(x)}\psi_0(x), \quad t \geq 0. \tag{2.5}$$

Choose $\tau > 0$ as the time step size and $t_n = n\tau$ for $n = 0, 1, \ldots$ as the time steps. Denote $\psi^{[n]}(x)$ to be the approximation of $\psi(x, t_n)$ for $n \geq 0$, then a second-order semi-discretization of the Schrödinger equation (2.1) via the Strang splitting can be given as [46]:

$$\psi^{[n+1]}(x) = \mathcal{S}_\tau(\psi^{[n]}) = e^{i\frac{\tau}{2}\Delta}e^{-i\varepsilon\tau V(x)}e^{i\frac{\tau}{2}\Delta}\psi^{[n]}(x),\ x \in \overline{\Omega}, \tag{2.6}$$

with $\psi^{[0]}(x) = \psi_0(x)$.

In space, we discretize the Schrödinger equation (2.1) by the Fourier pseudospectral method. Let N be an even positive integer and choose the spatial mesh size $h = (b - a)/N$, then the grid points are given as

$$x_j := a + jh, \quad j \in \mathcal{T}_N^0 = \{j \mid j = 0, 1, \ldots, N\}. \tag{2.7}$$

Denote $X_N := \{u = (u_0, u_1, \ldots, u_N)^T \in \mathbb{C}^{N+1} \mid u_0 = u_N\}$ with the l^∞-norm in X_N given as

$$\|u\|_{l^\infty} = \max_{0 \leq j \leq N-1} |u_j|, \quad u \in X_N. \tag{2.8}$$

Define $C_{\rm per}(\Omega) = \{u \in C(\overline{\Omega}) \mid u(a) = u(b)\}$ and

$$Y_N := \text{span}\left\{e^{i\mu_l(x-a)},\ x \in \overline{\Omega},\ l \in \mathcal{T}_N\right\},\ \mathcal{T}_N = \left\{l \mid l = -\frac{N}{2}, \ldots, \frac{N}{2} - 1\right\},$$

where $\mu_l = \frac{2\pi l}{b-a}$. For any $u(x) \in C_{\rm per}(\Omega)$ and a vector $u \in X_N$, let $P_N : L^2(\Omega) \to Y_N$ be the standard L^2-projection operator onto Y_N, $I_N : C_{\rm per}(\Omega) \to Y_N$ or $I_N :$

$X_N \to Y_N$ be the trigonometric interpolation operator [45], i.e.,

$$P_N u = \sum_{l\in\mathcal{T}_N} \widehat{u}_l e^{i\mu_l(x-a)}, \quad I_N u = \sum_{l\in\mathcal{T}_N} \widetilde{u}_l e^{i\mu_l(x-a)}, \quad x \in \overline{\Omega},$$

where

$$\widehat{u}_l = \frac{1}{b-a}\int_a^b u(x)e^{-i\mu_l(x-a)}dx, \quad \widetilde{u}_l = \frac{1}{N}\sum_{j=0}^{N-1} u_j e^{-i\mu_l(x_j-a)}, \quad l \in \mathcal{T}_N,$$

with u_j interpreted as $u(x_j)$ when involved.

Let ψ_j^n be the numerical approximation of $\psi(x_j,t_n)$ for $j \in \mathcal{T}_N^0$ and $n \geq 0$, and denote $\psi^n = (\psi_0^n, \psi_1^n, \ldots, \psi_N^n)^T \in X_N$ as the solution vector. Then, the time-splitting Fourier pseudospectral (TSFP) method for discretizing the Schrödinger equation (2.1) can be given for $n \geq 0$ as

$$\begin{aligned}
\psi_j^{(1)} &= \sum_{l\in\mathcal{T}_N} e^{-i\frac{\tau\mu_l^2}{2}} \widetilde{(\psi^n)}_l \, e^{i\mu_l(x_j-a)}, \\
\psi_j^{(2)} &= e^{-i\varepsilon\tau V(x_j)}\psi_j^{(1)}, \qquad\qquad j \in \mathcal{T}_N^0, \\
\psi_j^{n+1} &= \sum_{l\in\mathcal{T}_N} e^{-i\frac{\tau\mu_l^2}{2}} \widetilde{\left(\psi^{(2)}\right)}_l \, e^{i\mu_l(x_j-a)},
\end{aligned} \tag{2.9}$$

where $\psi_j^0 = \psi_0(x_j)$ for $j \in \mathcal{T}_N^0$.

Remark 2.1. The second-order Strang splitting is used for discretizing the Schrödinger equation (2.1). It is straightforward to design the first-order scheme via the Lie splitting and higher order scheme via a higher order splitting method, e.g., the fourth-order compact splitting method or partitioned Runge-Kutta splitting method [12, 43, 50].

2.2. **Local truncation error for the TSFP method.** For proving the (improved) uniform error bounds, we give some results for the local truncation error in this subsection.

We assume the exact solution $\psi(x,t)$ of the Schrödinger equation (2.1) up to the time $T_\varepsilon = T/\varepsilon$ for any $T > 0$ satisfies

$$\text{(A)} \quad \|\psi(x,t)\|_{L^\infty([0,T_\varepsilon];H^m_{\rm per})} \lesssim 1, \quad \|\partial_t\psi(x,t)\|_{L^\infty([0,T_\varepsilon];H^{m-2}_{\rm per})} \lesssim 1,$$

and the potential satisfies

$$\text{(B)} \quad V(x) \in H^{m^*}_{\rm per}, \quad m^* = \max\{m, 5\},$$

where m describes the regularity of the exact solution. Here, $H^m_{\rm per}(\Omega) = \{\phi \in H^m(\Omega) | \partial_x^k\phi(a) = \partial_x^k\phi(b),\ k = 0, 1, \ldots, m-1\}$, with the equivalent H^m-norm on $H^m_{\rm per}(\Omega)$ given as $\|\phi\|_{H^m} = \left(\sum_{l\in\mathbb{Z}} (1+\mu_l^2)^m |\widehat{\phi}_l|^2\right)^{1/2}$. In the rest of this paper, we may write $\psi(t) = \psi(x,t)$, i.e. omit the spatial variable, when there is no confusion. The following estimates of the local truncation error for the semi-discretization (2.6) hold.

Lemma 2.2. *Under assumptions* (A) *and* (B) *with* $m \geq 3$, *for* $0 < \varepsilon \leq 1$, *the local truncation error of the TSFP* (2.9) *for the Schrödinger equation with* $O(\varepsilon)$*-potential at time* t_n *can be written as* ($0 \leq n \leq T_\varepsilon/\tau - 1$)

$$\mathcal{E}^n(x) := P_N\mathcal{S}_\tau(P_N\psi(t_n)) - P_N\psi(t_{n+1}) = P_N\mathcal{F}(P_N\psi(t_n)) + R_n, \tag{2.10}$$

where

$$\mathcal{F}(P_N\psi(t_n)) = -i\varepsilon\tau f^n\left(\frac{\tau}{2}\right) + i\varepsilon\int_0^\tau f^n(s)\,ds, \tag{2.11}$$

with $f^n(s) = e^{i(\tau-s)\Delta}Ve^{is\Delta}P_N\psi(t_n)$, *and the following error estimates hold*

$$\|\mathcal{F}(P_N\psi(t_n))\|_{H^k} \lesssim \varepsilon\tau^3, \quad \|R_n\|_{H^k} \lesssim \varepsilon^2\tau^3 + \varepsilon\tau h^{m-k}, \quad k = 0, 1. \tag{2.12}$$

In addition, $\mathcal{E}^n(x), R_n(x) \in Y_N$ *and the* L^2*-estimates in* (2.12) *hold for* $m \geq 2$.

Proof. The proof is standard following [41, 42], and we sketch the procedure to emphasize the effects of spatial discretization and the parameter ε. By the Taylor expansion for $e^{-i\varepsilon\tau V}$, we have

$$\begin{aligned} P_N\left(\mathcal{S}_\tau(P_N\psi(t_n))\right) = e^{i\tau\Delta}P_N\psi(t_n) - i\varepsilon\tau P_N\left(e^{i\frac{\tau}{2}\Delta}Ve^{i\frac{\tau}{2}\Delta}P_N\psi(t_n)\right) \\ - \varepsilon^2\tau^2 P_N\left(\int_0^1 (1-\theta)e^{i\frac{\tau}{2}\Delta}e^{-i\varepsilon\theta\tau V}V^2e^{i\frac{\tau}{2}\Delta}P_N\psi(t_n)d\theta\right). \end{aligned}$$

On the other hand, by repeatedly using the Duhamel's principle, we can write

$$\begin{aligned} P_N\psi(t_{n+1}) = P_N\left(e^{i\tau\Delta}\psi(t_n)\right) - i\varepsilon P_N\left(\int_0^\tau e^{i(\tau-s)\Delta}Ve^{is\Delta}\psi(t_n)ds\right) \\ - \varepsilon^2 P_N\left(\int_0^\tau\int_0^s e^{i(\tau-s)\Delta}Ve^{i(s-w)\Delta}V\psi(t_n+w)dwds\right). \end{aligned}$$

Recalling assumptions (A) and (B), applying Fourier projections, we have

$$\begin{aligned} P_N\psi(t_{n+1}) = e^{i\tau\Delta}P_N\psi(t_n) - i\varepsilon\int_0^\tau P_N\left(e^{i(\tau-s)\Delta}Ve^{is\Delta}P_N\psi(t_n)\right)ds \\ - \varepsilon^2\int_0^\tau\int_0^s P_N\left(e^{i(\tau-s)\Delta}Ve^{i(s-w)\Delta}VP_N\psi(t_n+w)\right)dwds - r_h^n, \end{aligned}$$

with $\|r_h^n(x)\|_{L^2} \lesssim \varepsilon\tau h^m$ and $\|r_h^n(x)\|_{H^1} \lesssim \varepsilon\tau h^{m-1}$. Introducing $f^n(s)$ as in Lemma 2.2 and

$$B^n(s,w) = P_N\left(e^{i(\tau-s)\Delta}Ve^{i(s-w)\Delta}Ve^{iw\Delta}P_N\psi(t_n)\right),$$

the local truncation error can be written as [42]

$$\begin{aligned} \mathcal{E}^n = P_N\mathcal{F}(P_N\psi(t_n)) - \frac{\varepsilon^2\tau^2}{2}B^n\left(\frac{\tau}{2},\frac{\tau}{2}\right) + \varepsilon^2\int_0^\tau\int_0^s B^n(s,w)\,dwds \\ + \varepsilon^2 r_1^n + \varepsilon^2 r_2^n + r_h^n, \end{aligned}$$

where $\mathcal{F}(P_N\psi(t_n))$ is given in (2.11) and

$$\begin{aligned} r_1^n &= -\tau^2\int_0^1 (1-\theta)P_N\left(e^{i\frac{\tau}{2}\Delta}(e^{-i\varepsilon\theta\tau V}-1)V^2e^{i\frac{\tau}{2}\Delta}P_N\psi(t_n)\right)d\theta, \\ r_2^n &= \int_0^\tau\int_0^s\left(P_N\left(e^{i(\tau-s)\Delta}Ve^{i(s-w)\Delta}VP_N\psi(t_n+w)\right) - B^n(s,w)\right)dwds. \end{aligned}$$

Since $e^{i\tau\Delta}$ preserves the H^s-norm and $\|(e^{-i\varepsilon\theta\tau V}-1)V^2\|_{H^1} \lesssim \varepsilon\tau\theta\|V\|_{H^1}^3$, we have

$$\|r_1^n\|_{H^1} \lesssim \varepsilon\tau^3\|V\|_{H^1}^3\|\psi(t_n)\|_{H^1} \lesssim \varepsilon\tau^3.$$

The following estimates are standard (cf. [42]),

$$\|r_2^n\|_{H^1} \lesssim \varepsilon\tau^3\|V\|_{H^1}^2\,\|V\psi(\cdot)\|_{L^\infty([0,\tau];H^1)} \lesssim \varepsilon\tau^3,$$
$$\left\|-\frac{\tau^2}{2}B\left(\frac{\tau}{2},\frac{\tau}{2}\right)+\int_0^\tau\int_0^s B\left(s,w\right)dwds\right\|_{H^1} \lesssim \tau^3\|V\|_{H^3}^2\|\psi(t_n)\|_{H^3} \lesssim \tau^3.$$

Finally, for the major part of the local truncation error can be estimated by the midpoint quadrature rule as [42]

$$\|\mathcal{F}(P_N\psi(t_n))\|_{H^1} \lesssim \varepsilon\tau^3\|[\Delta,[\Delta,V]]P_N\psi(t_n)\|_{H^1} \lesssim \|V\|_{H^5}\|\psi(t_n)\|_{H^3}, \tag{2.13}$$

where $[\Delta,[\Delta,V]]$ is the double commutator. Thus, by setting

$$R_n = -\frac{\varepsilon^2\tau^2}{2}B^n\left(\frac{\tau}{2},\frac{\tau}{2}\right)+\varepsilon^2\int_0^\tau\int_0^s B^n\left(s,w\right)dwds+\varepsilon^2 r_1^n+\varepsilon^2 r_2^n+r_h^n, \tag{2.14}$$

we obtain the estimates in Lemma 2.2. □

2.3. **Uniform error bounds in L^2-norm.** In this subsection, we adopt the unitarity of the numerical solution flow in $L^2(\Omega)$ to establish the uniform error bound in L^2-norm with linear growth in t up to the time $t \le T_\varepsilon = T/\varepsilon$. We remark that the uniform estimates are standard, while the linear growth of the error only holds in the L^2-norm. The reason is that TSFP (2.9) only preserves the L^2-norm.

Theorem 2.3. *Let ψ^n be the numerical approximation obtained from the TSFP (2.9). Under assumptions (A) and (B) with $m \ge 2$, for any $0 < \varepsilon \le 1$, we have*

$$\|\psi(x,t_n) - I_N\psi^n\|_{L^2} \le (C_0 + C_1\varepsilon t_n)\tilde{C}(T)\left(h^m+\tau^2\right), \quad 0 \le n \le \frac{T/\varepsilon}{\tau}, \tag{2.15}$$

where C_0 and C_1 are two positive constants independent of h, τ, n, ε and T, $\tilde{C}(T)$ depends on $\|\psi\|_{L^\infty([0,T];H^m)}$ and $\|V\|_{H^{m^*}}$.

Proof. Noticing that

$$I_N\psi^n - \psi(t_n) = I_N\psi^n - P_N(\psi(t_n)) + P_N(\psi(t_n)) - \psi(t_n), \tag{2.16}$$

under assumptions (A) and (B), we get from the standard Fourier projection properties [45]

$$\|I_N\psi^n - \psi(t_n)\|_{L^2} \le \|I_N\psi^n - P_N(\psi(t_n))\|_{L^2} + C_2h^m,\ 0 \le n \le \frac{T/\varepsilon}{\tau}. \tag{2.17}$$

Thus, it suffices to consider the error function $e^n \in Y_N$ at t_n as

$$e^n := e^n(x) = I_N\psi^n - P_N\psi(t_n), \quad 0 \le n \le \frac{T/\varepsilon}{\tau}, \tag{2.18}$$

and $\left\|e^0\right\|_{L^2} \le C_3h^m$ implied by the standard projection and interpolation results. From the local error (2.10) in Lemma 2.2, we have the error equation for e^n ($0 \le n \le \frac{T/\varepsilon}{\tau}-1$),

$$e^{n+1} = I_N\psi^{n+1} - P_N\psi(t_{n+1}) = I_N\psi^{n+1} - P_N\mathcal{S}_\tau(P_N\psi(t_n)) + \mathcal{E}^n. \tag{2.19}$$

Noticing the fully discrete scheme (2.9) and $\mathcal{S}_\tau$ (2.6), i.e.

$$I_N\psi^{n+1} = e^{i\frac{\tau}{2}\Delta}(I_N\psi^{(2)}),\ I_N(\psi^{(2)}) = I_N(e^{-i\varepsilon\tau V(x)}\psi^{(1)}),\ I_N\psi^{(1)} = e^{i\frac{\tau}{2}\Delta}I_N\psi^n,$$
$$P_N(\mathcal{S}_\tau(\psi(t_n))) = e^{i\frac{\tau}{2}\Delta}(P_N\psi^{\langle 2\rangle}),\ \psi^{\langle 2\rangle} = e^{-i\varepsilon\tau V(x)}\psi^{\langle 1\rangle},\ \psi^{\langle 1\rangle} = e^{i\frac{\tau}{2}\Delta}P_N\psi(t_n),$$

in view of the facts that I_N and P_N are identical on Y_N and $e^{i\tau\Delta/2}$ preserves the H^k-norm ($k \geq 0$), using Taylor expansion $e^{-i\varepsilon\tau V(x)} = 1 - i\varepsilon\tau V(x)\int_0^1 e^{-i\varepsilon\theta\tau V(x)}\,d\theta$ and assumptions (A) and (B), we have

$$\|I_N\psi^{n+1} - P_N\mathcal{S}_\tau(P_N\psi(t_n))\|_{L^2} = \|I_N\psi^{\langle 2\rangle} - P_N\psi^{\langle 2\rangle}\|_{L^2}, \tag{2.20}$$

$$\|P_N\psi^{\langle 2\rangle} - I_N\psi^{\langle 2\rangle}\|_{L^2} = \left\|\varepsilon\tau(P_N - I_N)\left(V(x)\int_0^1 e^{-i\varepsilon\theta\tau V(x)}\,d\theta\psi^{\langle 1\rangle}\right)\right\|_{L^2}$$

$$\leq C_4\varepsilon\tau h^m, \tag{2.21}$$

where C_4 is obtained from Fourier interpolation and projection properties together with $\left\|\left(V(x)\int_0^1 e^{-i\varepsilon\theta\tau V(x)}\,d\theta\psi^{\langle 1\rangle}\right)\right\|_{H^m} \leq C(\|V\|_{H^m})\|\psi(t_n)\|_{H^m}$. In addition, by direct computation and Parseval's identity, we can derive

$$\begin{aligned}\|I_N\psi^{\langle 2\rangle} - I_N\psi^{\langle 2\rangle}\|_{L^2} &= \sqrt{h\sum_{j=0}^{N-1}|\psi_j^{\langle 2\rangle} - \psi^{\langle 2\rangle}(x_j)|^2} = \sqrt{h\sum_{j=0}^{N-1}|\psi_j^{\langle 1\rangle} - \psi^{\langle 1\rangle}(x_j)|^2}\\ &= \|I_N\psi^{\langle 1\rangle} - I_N\psi^{\langle 1\rangle}\|_{L^2} = \|I_N\psi^n - P_N\psi(t_n)\|_{L^2}\\ &= \|e^n\|_{L^2}. \end{aligned}\tag{2.22}$$

Taking the L^2-norm on both sides of (2.19) and combining (2.20),(2.21) and (2.22) together, in view of Lemma 2.2, we obtain for $0 \leq n \leq \frac{T/\varepsilon}{\tau} - 1$,

$$\begin{aligned}\|e^{n+1}\|_{L^2} &\leq \|\mathcal{E}^n\|_{L^2} + \|I_N\psi^{\langle 2\rangle} - P_N\psi^{\langle 2\rangle}\|_{L^2}\\ &\leq \|\mathcal{E}^n\|_{L^2} + \|I_N\psi^{\langle 2\rangle} - I_N\psi^{\langle 2\rangle}\|_{L^2} + \|P_N\psi^{\langle 2\rangle} - I_N\psi^{\langle 2\rangle}\|_{L^2}\\ &\leq \|e^n\|_{L^2} + C_5\left(\varepsilon\tau h^m + \varepsilon\tau^3\right).\end{aligned}\tag{2.23}$$

Thus, the following estimates hold

$$\|e^{n+1}\|_{L^2} \leq C_5\varepsilon t_{n+1}(h^m + \tau^2) + C_3h^m, \quad 0 \leq n \leq \frac{T/\varepsilon}{\tau} - 1, \tag{2.24}$$

and the conclusion of Theorem 2.3 by taking $C_0 = C_2 + C_3$ and $C_1 = C_5$ in view of (2.17). It is easy to verify all the constants appearing in the proof only depend on V and ψ. □

Remark 2.4. Regarding the estimate (2.15) in Theorem 2.3, $\tilde{C}(T)$ comes from the local truncation error, which depends on the growth of the Sobolev norm w.r.t. T in the assumption (A). Based on previous analytical results, $\tilde{C}(T)$ usually has a polynomial growth in T [15], and $\tilde{C}(T)$ could be uniformly bounded w.r.t. T for certain type of potential function $V(x)$ [51].

Remark 2.5. According to Theorem 2.3, the uniform error bound for the TSFP method in L^2-norm at time $t_\varepsilon = t/\varepsilon$ for the Schrödinger equation linearly grows with respect to t, and the results can be generalized to other splitting methods. In fact, given an accuracy bound $\delta_0 > 0$, the time (for simplicity, assume $\varepsilon = 1$ here) for the second-order splitting method to violate the accuracy requirement δ_0 is $O(\delta_0/\tau^2)$. For the first-order and fourth-order splitting methods, the time is $O(\delta_0/\tau)$ and $O(\delta_0/\tau^4)$, respectively. In other words, higher order splitting method performs much better in the long-time simulations not only regarding the higher accuracy but also longer simulation time to produce accurate solutions. For the L^2-estimates in Theorem 2.3, the regularity requirements on the potential $V(x)$ can be weakened. In addition, extensions to 2D/3D are straightforward.

Remark 2.6. By the similar procedure (or formally letting $h \to 0^+$), we could establish uniform error bounds for the semi-discretization. Let $\psi^{[n]}$ be the numerical approximation obtained from the Strang splitting (2.6). Under assumptions (A) and (B) with $m \geq 3$, for any $0 < \varepsilon \leq 1$, we have

$$\|\psi(x,t_n) - \psi^{[n]}\|_{L^2} \leq C_0 \varepsilon t_n \tau^2, \quad 0 \leq n \leq \frac{T/\varepsilon}{\tau}, \tag{2.25}$$

where C_0 is a positive constant independent of τ, n and ε. Such linear growth of the error constant w.r.t. t_n in (2.25) has been previously reported in [41].

2.4. **Improved uniform error bounds in H^1-norm.** In this subsection, we show improved uniform error bounds in H^1-norm for the Schrödinger equation with $O(\varepsilon)$-potential up to the time $T_\varepsilon = T/\varepsilon$ under assumptions (A) and (B) with $m \geq 3$, where we will work with H^1-estimates for the nonlinear case also to control the nonlinearity in 1D. It is worth noticing that in higher dimensions (2D/3D), H^2-estimates would be enough. The improved estimates rely on the cancellation phenomenon of non-resonant oscillating frequencies, for which we shall require the time step size τ to satisfy certain non-resonant conditions. In the fully discrete case, for the Fourier modes $|l| \leq \lceil \frac{1}{\tau_0} \rceil$ ($\tau_0 \in (0,1)$, $\lceil \cdot \rceil$ is the ceiling function), we impose the Diophantine type condition [29,44]: there exists a constant $C_0 > 0$ such that

$$\left|1 - e^{i\tau\mu_1^2 K}\right| \geq \frac{C_0 \tau^{\nu_1}}{(\mu_1^2|K|)^{\nu_2}}, \quad 0 < |K| \leq K_0 = \lceil 1/\tau_0 \rceil^2, \quad K \in \mathbb{Z}, \tag{2.26}$$

where $\nu_1 \in [0,1]$, $\nu_2 \geq -1$, and the bound $|K| \leq \lceil 1/\tau_0 \rceil^2$ corresponds to the interaction between potential $V(x)$ and the solution $\psi(x,t)$. In particular, we consider the following cases of time step sizes: for a given constant $\alpha \in (0,1)$, the time step size τ satisfies

$$\tau \in \left(0, \alpha \frac{2\pi}{\mu_1^2 (1+\tau_0)^2} \tau_0^2\right), \tag{2.27}$$

or the Diophantine type step condition [44]

$$\tau \in I_{\nu_3,\alpha,\tau_0} = \left\{ \tau > 0 : \left| \tau - \frac{2l\pi}{\mu_1^2 K} \right| \geq \frac{\lambda}{|\mu_1^2 K|^{2+\nu_3}}, K, l \in \mathbb{Z},\ 0 < |K| \leq K_0,\ 0 \leq l \right\}, \tag{2.28}$$

where $\lambda = \dfrac{\alpha\pi\mu_1^{2+2\nu_3}}{4\sum\limits_{k=1}^{\infty} 1/k^{1+\nu_3}}$ and $\nu_3 > 0$. (2.28) is adapted from a general form in [44], and it is direct to observe that

$$[0, 2\pi/\mu_1^2] \backslash I_{\nu_3,\alpha,\tau_0} = \bigcup_{0 \leq l \leq K, 1 \leq K \leq K_0} \left\{ \tau \in [0, 2\pi/\mu_1^2] : \left| \tau - \frac{2l\pi}{\mu_1^2 K} \right| < \frac{\lambda}{|\mu_1^2 K|^{2+\nu_3}} \right\},$$

where the Lebesgue measure of RHS is bounded by $\alpha\pi/(2\mu_1^2)$ and $I_{\nu_3,\alpha,\tau_0} \cap [0, 2\pi/\mu_1^2]$ has measure greater than $3\pi/2\mu_1^2$. Moreover, if $\tau \in I_{\nu_3,\alpha,\tau_0}$, $\tau + 2k\pi \in I_{\nu_3,\alpha,\tau_0}$ ($k \geq 0, k \in \mathbb{Z}$) and large time step sizes are admissible in (2.28).

Now we can verify that (2.27) fulfills (2.26) with $\nu_1 = 1, \nu_2 = -1, C_0 = \frac{\sin(\alpha\pi)}{\pi\alpha}$, while (2.28) fulfills (2.26) with $\nu_1 = 0, \nu_2 = 1 + \nu_3, C_0 = C_{\nu_3}\alpha$ (C_{ν_3} a constant depending on ν_3, see also (2.53)). (2.27) corresponds to the typical choice of time step size τ allowing $\tau \to 0^+$ and (2.28) allows ε dependent large time step size which is well suited for the long-time dynamics of Schrödinger equation (1.1). We remark here that similar non-resonance condition was used for establishing uniform

error bounds of time-splitting methods for the (nonlinear) Dirac equation in the nonrelativistic regime [7, 8]. We refer to Remark 2.11 for more discussions on the non-resonance condition (2.26).

Under the non-resonance condition (2.26), we have the following improved estimates.

Theorem 2.7. *Let ψ^n be the numerical approximation obtained from the TSFP (2.9). Under the assumptions (A) and (B) with $m \geq 3$, for any $\varepsilon \in (0, 1]$ and a fixed $\tau_0 \in (0, 1)$, when τ satisfies (2.27) or (2.28) ($m \geq 5 + 2\nu_3$ for (2.28) case), we have the estimates*

$$\|\psi(x, t_n) - I_N \psi^n\|_{H^1} \lesssim h^{m-1} + \varepsilon\tau^2 + \tau_0^{m-1}, \quad 0 \leq n \leq \frac{T/\varepsilon}{\tau}. \tag{2.29}$$

In particular, if the exact solution is smooth, i.e. $\psi(x, t) \in H^\infty_{\rm per}$, the τ_0^{m-1} part error would decrease exponentially in terms of τ_0 and can be ignored in practical computation when τ_0 is taken as $\tau_0^{\rm cr}$ (small but fixed, only depends on ψ and the logarithm of the machine precision), thus the improved error bounds for sufficiently small τ could be stated as

$$\|\psi(x, t_n) - I_N \psi^n\|_{H^1} \lesssim h^{m-1} + \varepsilon\tau^2, \quad 0 \leq n \leq \frac{T/\varepsilon}{\tau}. \tag{2.30}$$

Remark 2.8. Before the presentation of the proof, some observations are marked.

(1) First, $1/\tau_0 > 1$ serves as a cut-off mode, i.e. the modes $|l| > 1/\tau_0$ are treated by Fourier projection, and the modes $|l| \leq \lceil \frac{1}{\tau_0} \rceil$ will be treated by the RCO technique for non-resonant τ in (2.27)–(2.28).

(2) For (2.27), the requirement is that the step size τ resolves the largest oscillatory frequency of the free Schrödinger operator below the cut-off modes as $|\mu_l|^2 = \frac{4l^2\pi^2}{(b-a)^2} \sim \frac{4\pi^2}{(b-a)^2\tau_0^2}$, i.e. $\tau|\mu_l|^2 < 2\pi$. In turn, the error constant in front of $\varepsilon\tau^2$ depends on the parameter $\alpha \in (0, 1)$ (scales like $\frac{\alpha\pi}{\sin(\alpha\pi)}$). Thus, the introduced parameter τ_0 can be either fixed, or any other choices satisfying the condition $\tau < \alpha \frac{2\pi}{\mu_1^2(1+\tau_0)^2}\tau_0^2$, e.g. $\tau_0 = \frac{\sqrt{2}\mu_1}{\sqrt{\pi\alpha}}\sqrt{\tau}$. τ_0 serves as a Fourier projection parameter, similar to the role of the spatial mesh size h. Alternatively, we can also choose $\tau_0 = 2/N$ such that the last term in (2.29) could be controlled by the first term, and the requirement (2.27) on τ becomes a CFL type condition $\tau \lesssim h^2$.

(3) For the larger non-resonance step size τ in (2.28), Theorem 2.7 implies that for a given accuracy δ_0, τ can be chosen as $O(\sqrt{\delta_0}/\sqrt{\varepsilon})$ large, which is particularly superior for $\varepsilon \ll 1$. We notice that (2.28) requires higher regularity for deriving the improved error bounds.

(4) For general non-resonance time step sizes satisfying (2.26), the improved error estimates (2.29) hold by the similar arguments with slightly different regularity assumptions on the exact solution $\psi(x, t)$. Moreover, the error constant in front of the $\varepsilon\tau^2$ term depends on C_0 in (2.26) as $\sim 1/C_0$.

(5) For 2D/3D extensions, the improved error bounds can be directly established for the step sizes in (2.27) and non-resonance step sizes as (2.28) in higher dimensions. See Remark 2.9 for more details.

Proof. Following the proof of Theorem 2.3, we only need to estimate the error e^n in (2.18) for $0 \leq n \leq \frac{T/\varepsilon}{\tau}$. First, using the fact that $P_N = I_N$ when it is restricted

on Y_N, we can write for $0 \le n \le \frac{T/\varepsilon}{\tau}$,

$$I_N\psi^{n+1} - P_N\mathcal{S}_\tau(P_N\psi(t_n)) = e^{i\tau\Delta}\left(I_N\psi^n - P_N\psi(t_n)\right) + Q^n(x), \tag{2.31}$$

where $Q^n(x) \in Y_N$ is given by

$$\begin{aligned} Q^n(x) = &-i\varepsilon\tau e^{i\frac{\tau}{2}\Delta}\left(I_N\left(V(x)\int_0^1 e^{-i\varepsilon\theta\tau V(x)}\,d\theta\psi^{(1)}\right)\right) \\ &+ i\varepsilon\tau e^{i\frac{\tau}{2}\Delta}\left(P_N\left(V(x)\int_0^1 e^{-i\varepsilon\theta\tau V(x)}\,d\theta\psi^{\langle 1\rangle}\right)\right). \end{aligned} \tag{2.32}$$

Using Parseval's identity and finite difference operator (cf. [3,4]), by similar estimates (2.20), (2.21) and (2.22) for the L^2-norm case, we can control Q^n as

$$\|Q^n\|_{H^1} \lesssim \varepsilon\tau\left(h^{m-1} + \|e^n\|_{H^1}\right), \quad 0 \le n \le \frac{T/\varepsilon}{\tau} - 1. \tag{2.33}$$

From (2.31) and (2.19), we could derive that for $0 \le n \le \frac{T/\varepsilon}{\tau} - 1$,

$$e^{n+1} = e^{i\tau\Delta}e^n + Q^n(x) + \mathcal{E}^n, \tag{2.34}$$

which implies

$$e^{n+1} = e^{i(n+1)\tau\Delta}e^0 + \sum_{k=0}^{n} e^{i(n-k)\tau\Delta}\left(Q^k(x) + \mathcal{E}^k\right). \tag{2.35}$$

Step 1 (Identifying the leading error term). Using the local truncation error representation (2.12) in Lemma 2.2, we have

$$\sum_{k=0}^{n} e^{i(n-k)\tau\Delta}\mathcal{E}^k = \sum_{k=0}^{n} e^{i(n-k)\tau\Delta}(P_N\mathcal{F}(P_N\psi(t_k)) + R_k), \tag{2.36}$$

and

$$\left\|\sum_{k=0}^{n} e^{i(n-k)\tau\Delta}R_k\right\|_{H^1} \lesssim (n+1)\left(\varepsilon^2\tau^3 + \varepsilon\tau h^{m-1}\right) \lesssim T\varepsilon\tau^2 + Th^{m-1}, \tag{2.37}$$

$$\left\|\sum_{k=0}^{n} e^{i(n-k)\tau\Delta}Q^k(x)\right\|_{H^1} \lesssim \varepsilon\tau\sum_{k=0}^{n}\left\|e^k\right\|_{H^1} + h^{m-1}. \tag{2.38}$$

Combining above estimates and $\|e^0\|_{H^1} \lesssim h^{m-1}$, we obtain for $0 \le n \le \frac{T/\varepsilon}{\tau} - 1$,

$$\begin{aligned} \|e^{n+1}\|_{H^1} \lesssim\ & h^{m-1} + \varepsilon\tau^2 + \varepsilon\tau\sum_{k=0}^{n}\|e^k\|_{H^1} \\ &+ \left\|\sum_{k=0}^{n} e^{i(n-k)\tau\Delta}P_N\mathcal{F}(P_N\psi(t_k))\right\|_{H^1}. \end{aligned} \tag{2.39}$$

Recalling Lemma 2.2, we have $\|\mathcal{F}(P_N\psi(t_k))\|_{H^1} \lesssim \tau^3$, which implies $\|e^{n+1}\|_{H^1} \lesssim \tau^2 + h^{m-1}$. Thus, to prove the improved error estimates, we need analyze the last term in (2.39) carefully, i.e., treat the sum $\sum_{k=0}^{n} e^{i(n-k)\tau\Delta}P_N\mathcal{F}(P_N\psi(t_k))$ in a proper way. To gain an order of $O(\varepsilon)$ from the sum, we shall introduce the **regularity compensated oscillation** (RCO) technique. From (1.1), we find $\partial_t\psi(x,t) - i\Delta\psi(x,t) = O(\varepsilon)$, and it is natural to introduce the 'twisted variable' as

$$\phi(x,t) = e^{-it\Delta}\psi(x,t), \quad t \ge 0, \tag{2.40}$$

and $\phi(t) := \phi(x,t)$ satisfies the equation

$$i\partial_t \phi(x,t) = \varepsilon e^{-it\Delta}\left(V(x)e^{it\Delta}\phi(x,t)\right), \quad t>0. \tag{2.41}$$

It is direct to see that $\phi(x,t)$ enjoys the same H^k $(k\geq 0)$ bounds as $\psi(x,t)$, while

$$\|\partial_t \phi(t)\|_{H^m} \lesssim \varepsilon, \quad 0\leq t\leq T/\varepsilon. \tag{2.42}$$

The RCO approach would then perform a summation-by-parts procedure in the $\sum_{k=0}^{n} e^{i(n-k)\tau\Delta}P_N\mathcal{F}(P_N\psi(t_k))$ to force $\partial_t\phi(t)$ appear with a gain of order $O(\varepsilon)$, where τ is small to control the accumulation of the phase (frequency) of the type $e^{i(n-k)\tau\Delta}$. Since the number N of the spatial grid points could be very large, we shall introduce a cut-off parameter $\tau_0\in(0,1)$, where the high frequency modes $(|l|>\frac{1}{\tau_0})$ will be controlled by the smoothness of the exact solution and the Fourier projections, and the low frequency modes $(|l|\leq\frac{1}{\tau_0})$ will be dealt with the RCO technique.

Cut-off parameter. Choose $\tau_0\in(0,1)$, and let $N_0 = 2\lceil 1/\tau_0\rceil \in \mathbb{Z}^+$ with $1/\tau_0 \leq N_0/2 < 1+1/\tau_0$, then only those Fourier modes with $-\frac{N_0}{2}\leq l\leq \frac{N_0}{2}-1$ in $\mathcal{F}(P_N\psi(t_k))$ would be considered. Based on the Fourier projections and the assumption (A), we have $\|P_{N_0}\psi(x,t)-P_N\psi(x,t)\|_{L^\infty([0,T/\varepsilon];H^1)}\lesssim h^{m-1}+N_0^{1-m}\lesssim h^{m-1}+\tau_0^{m-1}$ and for $0\leq n\leq\frac{T/\varepsilon}{\tau}-1$,

$$\|P_{N_0}\mathcal{F}(P_{N_0}\psi(t_n))-P_N\mathcal{F}(P_N\psi(t_n))\|_{H^1}\lesssim \varepsilon\tau(h^{m-1}+\tau_0^{m-1}). \tag{2.43}$$

Indeed, since $P_N\psi(t_k)\in Y_N$, we could actually assume the choice of τ_0 such that $N_0\leq N$, but here we work without this condition for the convenience of extension to the semi-discretization-in-time case.

Based on (2.39), (2.40) and (2.43), recalling the unitary properties of $e^{it\Delta}$, we find for $0\leq n\leq\frac{T/\varepsilon}{\tau}-1$,

$$\left\|e^{n+1}\right\|_{H^1}\lesssim h^{m-1}+\tau_0^{m-1}+\varepsilon\tau^2+\varepsilon\tau\sum_{k=0}^{n}\left\|e^k\right\|_{H^1}+\|\mathcal{R}^n\|_{H^1}, \tag{2.44}$$

$$\mathcal{R}^n(x)=\sum_{k=0}^{n}e^{-i(k+1)\tau\Delta}P_{N_0}\mathcal{F}(e^{it_k\Delta}(P_{N_0}\phi(t_k))). \tag{2.45}$$

Step 2 (Analysis via RCO). Let $\phi(t)=\sum_{l\in\mathbb{Z}}\widehat{\phi}_l(t)e^{i\mu_l(x-a)}$ $(t\geq 0)$, and we have $P_{N_0}\phi(t)=\sum_{l\in\mathcal{T}_{N_0}}\widehat{\phi}_l(t)e^{i\mu_l(x-a)}$, where $\widehat{\phi}_l(t)$ is the l-th Fourier coefficient of $\phi(x,t)$. For $l\in\mathcal{T}_{N_0}$, introduce the multi-index set $\mathcal{I}_l^{N_0}$ associated with l as

$$\mathcal{I}_l^{N_0}=\{(l_1,l_2)\mid l_1+l_2=l,\ l_1\in\mathbb{Z},\ l_2\in\mathcal{T}_{N_0}\}. \tag{2.46}$$

According to the definition of $\mathcal{F}$ in Lemma 2.2, we have the expansion

$$e^{-i(k+1)\tau\Delta}P_{N_0}\left(e^{i(\tau-s)\Delta}Ve^{is\Delta}P_{N_0}\psi(t_n)\right)=\sum_{l\in\mathcal{T}_{N_0}}\sum_{(l_1,l_2)\in\mathcal{I}_l^{N_0}}\mathcal{G}_{k,l,l_1,l_2}(s)e^{i\mu_l(x-a)},$$

where $\mathcal{G}_{k,l,l_1,l_2}(s)$ $(l,l_2\in\mathcal{T}_{N_0})$ is a function of s as

$$\mathcal{G}_{k,l,l_1,l_2}(s)=e^{i(t_k+s)\delta_{l,l_2}}\widehat{V}_{l_1}\widehat{\phi}_{l_2}(t_k),\quad \delta_{l,l_2}=\delta_l-\delta_{l_2},\quad \delta_l=\mu_l^2. \tag{2.47}$$

Then, the remainder term $\mathcal{R}^n(x)$ in (2.44) reads

$$\mathcal{R}^n(x)=i\varepsilon\sum_{k=0}^{n}\sum_{l\in\mathcal{T}_{N_0}}\sum_{(l_1,l_2)\in\mathcal{I}_l^{N_0}}\lambda_{k,l,l_1,l_2}e^{i\mu_l(x-a)}, \tag{2.48}$$

where the coefficients λ_{k,l,l_1,l_2} are given by

$$\lambda_{k,l,l_1,l_2} = -\tau \mathcal{G}_{k,l,l_1,l_2}(\tau/2) + \int_0^\tau \mathcal{G}_{k,l,l_1,l_2}(s)\, ds = r_{l,l_2} e^{it_k \delta_{l,l_2}} c_{k,l,l_1,l_2}, \tag{2.49}$$

and

$$\begin{aligned} c_{k,l,l_1,l_2} &= \widehat{V}_{l_1} \widehat{\phi}_{l_2}(t_k), \\ r_{l,l_2} &= -\tau e^{i\frac{\tau \delta_{l,l_2}}{2}} + \int_0^\tau e^{is\delta_{l,l_2}}\, ds = O(\tau^3 (\delta_{l,l_2})^2). \end{aligned} \tag{2.50}$$

The key observation from (2.50) is: if $\delta_{l,l_2} = 0$, $r_{l,l_2} = 0$ and the term λ_{k,l,l_1,l_2} in (2.49) vanishes. Thus, in the discussion below, we shall assume that $\delta_{l,l_2} \neq 0$. Based on the RCO, we will go through the detailed structure of (2.48) and exchange the order of summation (sum over index k first), which will result in the terms like $\phi(t_k) - \phi(t_{k+1}) = O(\tau \partial_t \phi) = O(\varepsilon\tau)$ to gain an order of ε.

First, for $l \in \mathcal{T}_{N_0}$ and $(l_1, l_2) \in \mathcal{I}_l^{N_0}$, we have

$$|\delta_{l,l_2}| \leq \delta_{N_0/2} = \mu_{N_0/2}^2 = (\pi N_0)^2/(b-a)^2 \leq \frac{4\pi^2(1+\tau_0)^2}{\tau_0^2 (b-a)^2} = \frac{\mu_1^2 (1+\tau_0)^2}{\tau_0^2}, \tag{2.51}$$

which implies the following estimates for the case (2.27) ($0 < \tau \leq \alpha \frac{2\pi}{\mu_1^2(1+\tau_0)^2} \tau_0^2$ with $\alpha \in (0,1)$ and $\tau_0 \in (0,1)$)

$$\frac{\tau}{2} |\delta_{l,l_2}| < \alpha\pi, \tag{2.52}$$

and for the case (2.28), we have

$$\left| \frac{\tau}{2} |\delta_{l,l_2}| - k\pi \right| \geq \frac{\lambda}{2|\delta_{l,l_2}|^{1+\nu_3}}, \quad k = \lceil \frac{|\delta_{l,l_2}|\tau}{2\pi} \rceil, \lceil \frac{|\delta_{l,l_2}|\tau}{2\pi} \rceil - 1, \tag{2.53}$$

where $\frac{\lambda}{2|\delta_{l,l_2}|^{1+\nu_3}} \leq \frac{\alpha\pi}{8} \leq \frac{\pi}{8}$ and $\sin\left(\frac{\lambda}{2|\delta_{l,l_2}|^{1+\nu_3}}\right) \geq \frac{\lambda}{4|\delta_{l,l_2}|^{1+\nu_3}}$ ($\sin(s) \geq \frac{s}{2}$ if $s \in (0, \pi/3)$).

Denoting $S_{n,l,l_2} = \sum_{k=0}^{n} e^{it_k \delta_{l,l_2}}$ ($n \geq 0$) and using summation-by-parts, we find from (2.49) that

$$\sum_{k=0}^{n} \lambda_{k,l,l_1,l_2} = r_{l,l_2} \sum_{k=0}^{n-1} S_{k,l,l_2} (c_{k,l,l_1,l_2} - c_{k+1,l,l_1,l_2}) + S_{n,l,l_2}\, r_{l,l_2}\, c_{n,l,l_1,l_2}, \tag{2.54}$$

and

$$c_{k,l,l_1,l_2} - c_{k+1,l,l_1,l_2} = \widehat{V}_{l_1} \left(\widehat{\phi}_{l_2}(t_k) - \widehat{\phi}_{l_2}(t_{k+1}) \right). \tag{2.55}$$

For the step size (2.27), we know from (2.52) that

$$|S_{n,l,l_2}| \leq \frac{2}{|1 - e^{i\tau\delta_{l,l_2}}|} = \frac{1}{|\sin(\tau\delta_{l,l_2}/2)|} \leq \frac{C}{\tau |\delta_{l,l_2}|}, \quad \forall n \geq 0, \tag{2.56}$$

where we have used the fact $\frac{\sin(s)}{s}$ is bounded (decreasing) for $s \in [0, \alpha\pi)$ and $C = \frac{2\alpha\pi}{\sin(\alpha\pi)}$ (noticing the case $\delta_{l,l_2} = 0$ is trivial and δ_{l,l_2} is assumed to be nonzero here). Combining (2.50), (2.54), (2.55) and (2.56), we have

$$\left| \sum_{k=0}^{n} \lambda_{k,l,l_1,l_2} \right| \lesssim \tau^2 |\delta_{l,l_2}| \left| \widehat{V}_{l_1} \right| \left[\sum_{k=0}^{n-1} \left| \widehat{\phi}_{l_2}(t_k) - \widehat{\phi}_{l_2}(t_{k+1}) \right| + \left| \widehat{\phi}_{l_2}(t_n) \right| \right]. \tag{2.57}$$

We note that (2.57) is the key for the refined estimate, where we shall gain an order of ε from the $\phi(t_k) - \phi(t_{k+1})$ terms (see (2.42)). Of course, the condition (2.52) is also important to exclude the resonance case where S_n could be unbounded, i.e., (2.52) makes the estimate (2.57) available. For the non-resonance step size (2.28), we can similarly obtain $|S_{n,l,l_2}| \leq 1/\sin(\lambda/2|\delta_{l,l_2}|^{1+\nu_3}) \leq \frac{4|\delta_{l,l_2}|^{1+\nu_3}}{\lambda} = \tilde{C}|\delta_{l,l_2}|^{1+\nu_3}/\alpha$ for some constant $\tilde{C} > 0$. Then, by noticing $|r_{l,l_2}| = O(\tau^2\delta_{l,l_2})$, the simialr estimates in (2.57) hold as

$$\left|\sum_{k=0}^{n}\lambda_{k,l,l_1,l_2}\right| \lesssim \tau^2|\delta_{l,l_2}|^{2+\nu_3}\left|\widehat{V}_{l_1}\right|\left[\sum_{k=0}^{n-1}\left|\widehat{\phi}_{l_2}(t_k)-\widehat{\phi}_{l_2}(t_{k+1})\right|+\left|\widehat{\phi}_{l_2}(t_n)\right|\right].$$

Since the rest arguments are almost the same for both step sizes (2.27) and (2.28) (regularities are different), we shall only treat the case (2.27) below.

Step 3 (Improved estimates). Now, we are ready to give the improved estimates. For $l \in \mathcal{T}_{N_0}$ and $(l_1, l_2) \in \mathcal{I}_l^{N_0}$, simple calculations show ($l = l_1 + l_2$)

$$1+\mu_l^2 \leq (1+\mu_{l_1}^2)(1+\mu_{l_2}^2), \quad |\delta_{l,l_2}| \leq (1+\mu_{l_1}^2)(1+\mu_{l_2}^2). \tag{2.58}$$

Based on (2.48), (2.57) and (2.58), using Cauchy inequality, we now estimate the remainder term in (2.44),

(2.59)

$$\begin{aligned}
&\|\mathcal{R}^n(x)\|_{H^1}^2\\
&= \varepsilon^2\sum_{l\in\mathcal{T}_{N_0}}(1+\mu_l^2)\Big|\sum_{(l_1,l_2)\in\mathcal{I}_l^{N_0}}\sum_{k=0}^{n}\lambda_{k,l,l_1,l_2}\Big|^2\\
&\lesssim \varepsilon^2\tau^4\Bigg\{\sum_{l\in\mathcal{T}_{N_0}}\Bigg(\sum_{(l_1,l_2)\in\mathcal{I}_l^{N_0}}\left|\widehat{V}_{l_1}\right|\left|\widehat{\phi}_{l_2}(t_n)\right|\prod_{j=1}^{2}(1+\mu_{l_j}^2)^{3/2}\Bigg)^2\\
&\quad + n\sum_{k=0}^{n-1}\Bigg[\sum_{l\in\mathcal{T}_{N_0}}\Bigg(\sum_{(l_1,l_2)\in\mathcal{I}_l^{N_0}}\left|\widehat{V}_{l_1}\right|\left|\widehat{\phi}_{l_2}(t_k)-\widehat{\phi}_{l_2}(t_{k+1})\right|\prod_{j=1}^{2}(1+\mu_{l_j}^2)^{3/2}\Bigg)^2\Bigg]\Bigg\}.
\end{aligned}$$

To estimate each term in (2.59), we use the auxiliary function $\xi(x) = \sum_{l\in\mathbb{Z}}(1+\mu_l^2)^{3/2}\left|\widehat{\phi}_l(t_n)\right|e^{i\mu_l(x-a)}$, where $\xi(x) \in H_{\rm per}^{m-3}(\Omega)$ implied by the assumption (A) and $\|\xi(x)\|_{H^s} \lesssim \|\phi(t_n)\|_{H^{s+3}}$ ($s \leq m-3$). Similarly, introduce the function $U(x) = \sum_{l\in\mathbb{Z}}(1+\mu_l^2)^{3/2}\left|\widehat{V}_l\right|e^{i\mu_l(x-a)}$, where $U(x) \in H_{\rm per}^2$ implied by the assumption (B). Expanding

$$U(x)\xi(x) = \sum_{l\in\mathbb{Z}}\sum_{l_1+l_2=l}\prod_{j=1}^{2}(1+\mu_{l_j}^2)^{3/2}\left|\widehat{V}_{l_1}\right|\left|\widehat{\phi}_{l_2}(t_n)\right|e^{i\mu_l(x-a)},$$

we could obtain

$$\begin{aligned}
&\sum_{l\in\mathcal{T}_{N_0}}\Bigg(\sum_{(l_1,l_2)\in\mathcal{I}_l^{N_0}}\left|\widehat{V}_{l_1}\right|\left|\widehat{\phi}_{l_2}(t_n)\right|\prod_{j=1}^{2}(1+\mu_{l_j}^2)^{3/2}\Bigg)^2\\
&\leq \|U(x)\xi(x)\|_{L^2}^2 \lesssim \|V(x)\|_{H^4}^2\|\phi(t_k)\|_{H^3}^2 \lesssim 1,
\end{aligned} \tag{2.60}$$

which together with (2.42) implies (applying the same trick to the rest terms) for $0 \le n \le \frac{T/\varepsilon}{\tau} - 1$,

$$\begin{aligned}\|\mathcal{R}^n(x)\|_{H^1}^2 &\lesssim \varepsilon^2\tau^4\Big(\|\phi(t_k)\|_{H^3}^2 + n\sum_{k=0}^{n-1}\|\phi(t_k)-\phi(t_{k+1})\|_{H^3}^2\Big)\\ &\lesssim \varepsilon^2\tau^4 + n^2\varepsilon^4\tau^6\|\partial_t\phi(x,t)\|_{L^\infty([0,T_\varepsilon];H^3)}^2 \lesssim \varepsilon^2\tau^4.\end{aligned} \tag{2.61}$$

Combining (2.44) and (2.61), we have

$$\|e^{n+1}\|_{H^1} \lesssim h^{m-1} + \tau_0^{m-1} + \varepsilon\tau^2 + \varepsilon\tau\sum_{k=0}^{n}\|e^k\|_{H^1}, \quad 0 \le n \le \frac{T/\varepsilon}{\tau} - 1. \tag{2.62}$$

Discrete Gronwall's inequality would yield $\|e^{n+1}\|_{H^1} \lesssim h^{m-1}+\varepsilon\tau^2+\tau_0^{m-1}$ ($0 \le n \le \frac{T/\varepsilon}{\tau} - 1$), and the proof for the improved uniform error bound (2.15) in Theorem 2.7 is completed. □

Remark 2.9. From the proof, the key steps of RCO are the cut-off (2.43) to separate the high/low Fourier modes, sufficiently small time step size τ (2.27) (or non-resonance step size (2.28)) to compensate the growth of errors at low Fourier modes via expansion (cf. (2.52),(2.56) and (2.57)), and the estimates of the Fourier coefficients (cf. (2.61)). Here, the special structure of the Fourier functions is important, e.g. $e^{i\mu_l(x-a)}e^{i\mu_k(x-a)} = e^{i\mu_{l+k}(x-a)}$. Based on above observations, it is straightforward to extend the RCO analysis to higher dimensions (2D/3D) in rectangular domain with periodic boundary conditions for the sufficiently small time step sizes ((2.27) type), as the higher dimensional tensor Fourier basis enjoys the same properties ensuring the Fourier expansion for products of periodic functions. Notice that in 2D/3D for rectangular domains with irrational aspect ratios, the higher dimensional version of the non-resonance step size (2.28) is difficult to check, while the (2.27) type condition always holds for sufficiently small τ.

Remark 2.10. In the proof, (2.52), (2.56) and (2.57) suggest the two order spatial regularity is regained from the summation-by-parts process indicated by $1/(\tau\delta_{l,l_2})$ (δ_{l,l_2} is roughly Δ). Usually, such gained regularity will be lost when considering the other term of the summation-by-parts, i.e. the terms corresponding to $\phi(t_k) - \phi(t_{k+1}) = O(\tau\partial_t\phi)$, where ∂_t term will compensate the regularity gain from δ_{l,l_2}. However, as we have chosen a particularly designed twisted variable $\phi(t)$, there will be no regularity loss in $\phi(t_k) - \phi(t_{k+1})$, but with a gain of order ε.

Remark 2.11. Passing $h \to 0^+$ in Theorem 2.7, we can recover the estimates in the semi-discrete-in-time case, and it would be interesting to derive the estimates involving τ and h only, i.e. $O(h^{m-1}+\varepsilon\tau^2)$ without the parameter τ_0. The following two cases are included:

(1) Non-resonance τ. Since the free Schrödiner operator $e^{it\Delta}$ is periodic in t, we could impose the following Diophantine condition [29, 44]: there exist $\gamma > 0$ and $\nu > 1$ such that

$$\left|\frac{1 - e^{i\tau\mu_1^2 K}}{\tau}\right| \ge \frac{\gamma}{|K|^\nu}, \quad \forall K \in \mathbb{Z},\ K \ne 0, \tag{2.63}$$

which is a common choice allowing $\tau \to 0^+$. In particular, one can choose τ similar to (2.28) as [44]

$$\left\{\tau \in (0,1) : \left|\tau - \frac{2l\pi}{\mu_1^2 K}\right| \geq \frac{\lambda}{|l|^{\tilde{\nu}_1}|K|^{\tilde{\nu}_2}}, K, l \in \mathbb{Z},\ 1 \leq l, |K|\right\}, \tag{2.64}$$

where $\tilde{\nu}_1 \in [-1,1]$ and $\tilde{\nu}_1 + \tilde{\nu}_2 > 2$, and $\lambda > 0$ is a small constant. The above set (2.64) is nowhere dense and hence not easy to verify in practice for a particular choice of τ. Once the non-resonance condition (2.63) is satisfied, the improved estimates in Theorem 2.7 hold and (2.26) holds for any $\tau_0 \in (0,1)$. Therefore, we can simply take the limit as $\tau_0 \to 0^+$ to derive the improved error bounds at $O(\varepsilon\tau^2 + h^{m-1})$ for the above non-resonance step sizes.

(2) Sufficiently small τ with the constraint $\tau \lesssim C_\varepsilon$ for some ε dependent C_ε (this type step size τ may not be included in (2.63)). Following the proof of Theorem (2.7), we can fix $\tau_0 = C\sqrt{\tau}$ for some constant C. By optimizing the error bounds $O(\varepsilon\tau^2 + \tau_0^{m-1}) = O(\varepsilon\tau^2 + C^{m-1}\tau^{(m-1)/2})$, we find that the $O(\varepsilon\tau^2 + h^{m-1})$ error bound would hold for sufficiently small $\tau \lesssim \varepsilon^{2/(m-5)}$ when $m > 5$. If the exact solution $\psi(x,t)$ is sufficiently smooth with Fourier coefficient $\hat{\psi}_l(t) \sim O(e^{-c|l|})$ $(c > 0,\ |l| \gg 1)$ decaying exponentially fast, the projection error due to the τ_0 cut-off would be $O(e^{-\tilde{C}/\sqrt{\tau}})$ and the error bounds become $O(\varepsilon\tau^2 + h^{m-1})$ when $\tau \lesssim 1/|\ln\varepsilon|$ $(\varepsilon \in (0,1))$. Therefore, $C_\varepsilon = \varepsilon^{2/(m-5)}$ for sufficiently smooth solutions with $m > 5$ and $C_\varepsilon = 1/|\ln\varepsilon|$ for the solutions with exponentially decaying Fourier coefficients.

2.5. **Numerical results.** In this subsection, we present numerical results of the TSFP method for the long-time dynamics of the Schrödinger equation with $O(\varepsilon)$-potential in 1D, up to the time $T_\varepsilon = \frac{T}{\varepsilon}$.

First, we show an example to confirm that the uniform error bound in L^2-norm linearly grows with respect to T. We choose the potential $V(x) = 5\cos(2\pi x)$ and the $H^2_{\rm per}$ initial data as

$$\psi_0(x) = 5x^2(1-x)^2, \quad x \in [0,1]. \tag{2.65}$$

The regularity is enough to ensure the uniform and the improved error bounds in L^2-norm. The 'exact' solution $\psi(x,t)$ is obtained numerically by the TSFP (2.9) with a very fine mesh size $h_e = 1/128$ and time step size $\tau_e = 10^{-4}$. To quantify the error, we introduce the following error functions:

$$e_{L^2}(t_n) = \|\psi(x,t_n) - I_N\psi^n\|_{L^2}, \quad e_{H^1}(t_n) = \|\psi(x,t_n) - I_N\psi^n\|_{H^1}, \tag{2.66}$$

and

$$e_{L^2,\max}(t_n) = \max_{0\leq q\leq n} e_{L^2}(t_q), \quad e_{H^1,\max}(t_n) = \max_{0\leq q\leq n} e_{H^1}(t_q).$$

In the rest of the paper, the spatial mesh size is always chosen sufficiently small and thus spatial errors can be ignored when considering the long time error growth and/or the temporal errors.

Figure 1 plots the long-time errors in L^2-norm of the TSFP method for the Schrödinger equation (2.1) with $\varepsilon = 1$ and different time step τ, which shows that the uniform errors in L^2-norm linearly grows with respect to the time. In addition, for a given accuracy bound, the time to exceed the error bar is quadruple when the time step is half, which also confirms the linear growth. For comparisons, Figure 2 depicts the long-time errors in L^2-norm of the fourth-order time-splitting method, which indicates that higher order time-splitting methods could get better accuracy

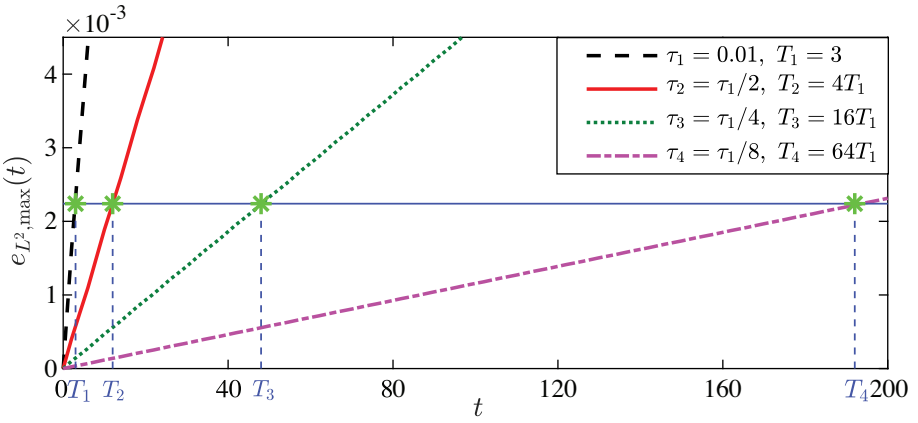

FIGURE 1. Long-time temporal errors in L^2-norm of the TSFP (2.9) for the Schrödinger equation (2.1) with $\varepsilon = 1$ and different time step τ

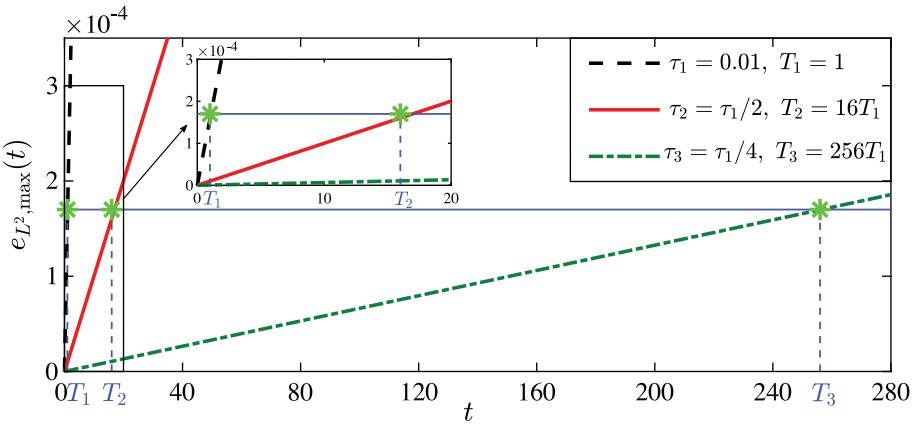

FIGURE 2. Long-time temporal errors in L^2-norm of the fourth-order time-splitting method for the Schrödinger equation (2.1) with $\varepsilon = 1$ and different time step τ

with the same time step size as well as longer time simulations within a given accuracy bound.

Next, we report the convergence test for the Schrödinger equation (2.1) with the potential $V(x) = \sin(x)$ and the smooth initial data

$$\psi_0(x) = 2/(2 + \sin^2(x)), \quad x \in [0, 2\pi]. \tag{2.67}$$

The 'exact' solution $\psi(x,t)$ is obtained numerically by the TSFP (2.9) with $h_e = \pi/64$ and $\tau_e = 10^{-4}$.

Figure 3 displays the long-time errors in H^1-norm of the TSFP method for the Schrödinger equation (2.1) with the fixed time step τ and different ε, which confirms the improved uniform error bound in H^1-norm at $O(\varepsilon\tau^2)$ up to the $O(1/\varepsilon)$ time. Figures 4 and 5 exhibit the spatial and temporal errors of the TSFP (2.9) for the

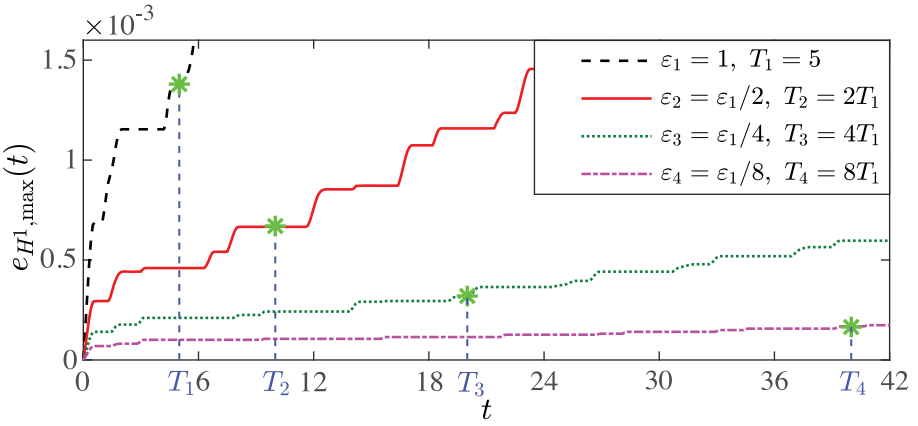

FIGURE 3. Long-time temporal errors in H^1-norm of the TSFP (2.9) for the Schrödinger equation (2.1) with different ε

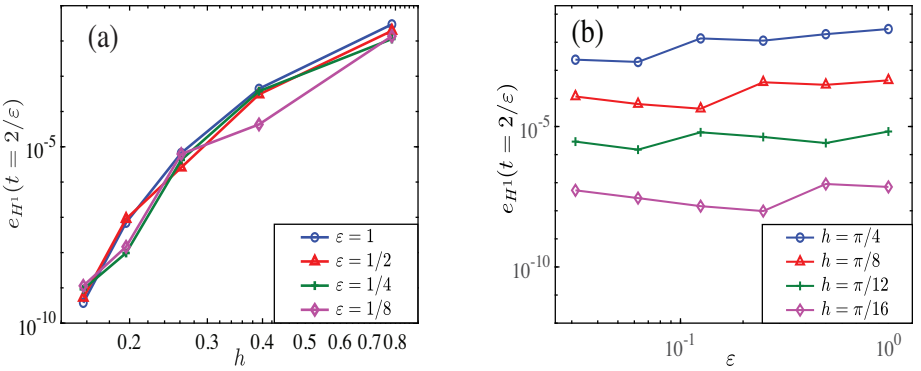

FIGURE 4. Long-time spatial errors in H^1-norm of the TSFP (2.9) for the Schrödinger equation (2.1) at $t = 2/\varepsilon$

Schrödinger equation (2.1) at $t = \frac{2}{\varepsilon}$. Each line in Figure 4 (a) shows the spectral accuracy of the TSFP method in space and Figure 4 (b) verifies the spatial errors are independent of the small parameter ε in the long-time regime. Figure 5 (a) shows the second-order convergence of the TSFP method in time. Each line in Figure 5 (b) gives the global errors in H^1-norm with a fixed time step τ and verifies that the global error performs like $O(\varepsilon\tau^2)$ up to the $O(1/\varepsilon)$ time.

Figure 6 displays the long-time errors of the TSFP method for the Schrödinger equation (2.1) with large time step size. Each line in Figure 6 (a) plots the long-time errors with the time step sizes $\tau = O(1/\sqrt{\varepsilon})$, which are almost constants for different ε, confirming the error bound (2.29). In Figure 6 (b), we choose the time step size satisfying the non-resonance condition, and Figure 6 (b) shows the improved uniform error bounds with large time step size.

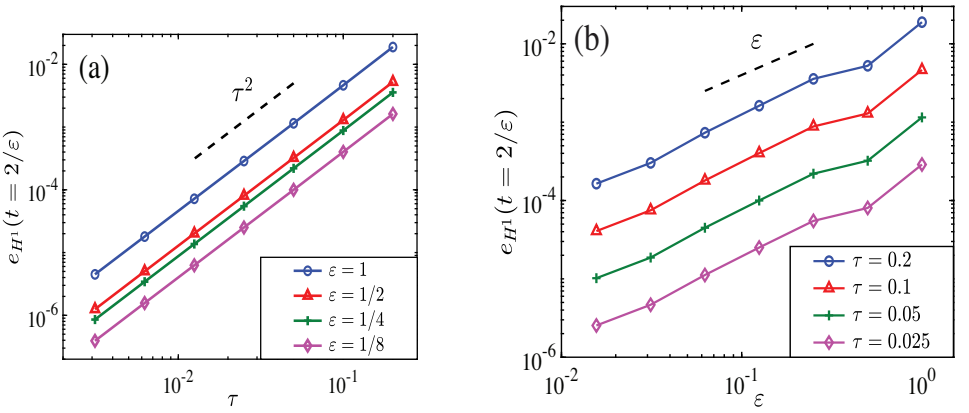

FIGURE 5. Long-time temporal errors in H^1-norm of the TSFP (2.9) for the Schrödinger equation (2.1) at $t = 2/\varepsilon$

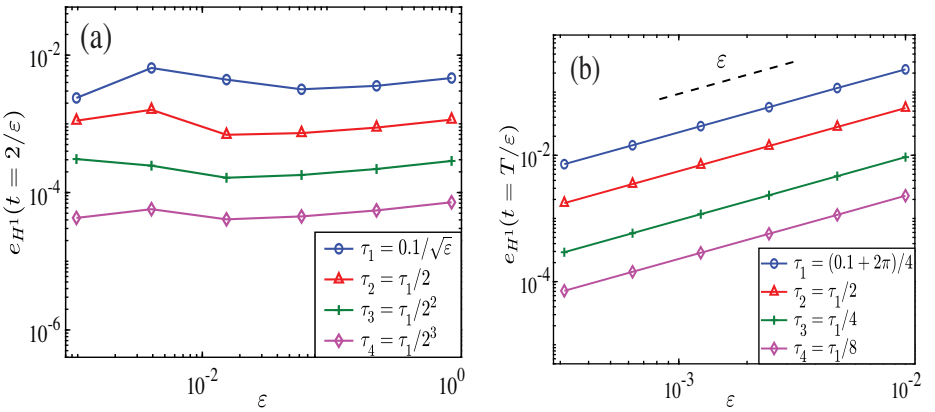

FIGURE 6. Long-time temporal errors in H^1-norm of the TSFP (2.9) for the Schrödinger equation (2.1) with large time step size

3. Improved uniform error bounds for the NLSE

In this section, we adopt the TSFP method to solve the NLSE with weak nonlinearity and extend the technique of regularity compensation oscillation (RCO) to obtain improved uniform error bounds for the cubic NLSE with $O(\varepsilon^2)$-nonlinearity up to the $O(1/\varepsilon^2)$ time.

3.1. **The TSFP method.** We present the TSFP method for the NLSE (1.2) in 1D and extensions to higher dimensions are straightforward (see also Remark 2.9). In 1D, the NLSE (1.2) with initial data (1.3) and periodic boundary conditions on $\Omega = (a, b)$ collapses to

$$\begin{cases} i\partial_t\psi(x,t) = -\Delta\psi(x,t) \pm \varepsilon^2|\psi(x,t)|^2\psi(x,t), \quad a < x < b,\ t > 0, \\ \psi(a,t) = \psi(b,t),\ \partial_x\psi(a,t) = \partial_x\psi(b,t),\ t \geq 0, \\ \psi(x,0) = \psi_0(x),\ x \in [a,b]. \end{cases} \tag{3.1}$$

By the same time-splitting technique as that in the linear case, the semi-discretization of the NLSE (3.1) via the Strang splitting is given as:

$$\psi^{[n+1]}(x) = \mathcal{S}_\tau(\psi^{[n]}) = e^{i\frac{\tau}{2}\Delta} e^{\mp i\varepsilon^2\tau\left|e^{i\frac{\tau}{2}\Delta}\psi^{[n]}(x)\right|^2} e^{i\frac{\tau}{2}\Delta}\psi^{[n]}(x), \quad x \in \Omega, \tag{3.2}$$

with $\psi^{[0]}(x) = \psi_0(x)$. Respectively, the full-discretization for the NLSE (3.1) can be written as

$$\begin{aligned} \psi_j^{(1)} &= \sum_{l\in\mathcal{T}_N} e^{-i\frac{\tau\mu_l^2}{2}} \widetilde{(\psi^n)}_l \, e^{i\mu_l(x_j-a)}, \\ \psi_j^{(2)} &= e^{\mp i\varepsilon^2\tau\lambda|\psi_j^{(1)}|^2}\psi_j^{(1)}, \qquad\qquad j \in \mathcal{T}_N^0, \quad n \geq 0, \\ \psi_j^{n+1} &= \sum_{l\in\mathcal{T}_N} e^{-i\frac{\tau\mu_l^2}{2}} \widetilde{\left(\psi^{(2)}\right)}_l \, e^{i\mu_l(x_j-a)}, \end{aligned} \tag{3.3}$$

where $\psi_j^0 = \psi_0(x_j)$ for $j \in \mathcal{T}_N^0$.

3.2. **Improved uniform error bounds in H^1-norm.** For the NLSE, we assume the exact solution $\psi(x,t)$ up to the time at $T_\varepsilon = T/\varepsilon^2$ with $T > 0$ fixed satisfies:

$$\text{(C)} \qquad \|\psi(x,t)\|_{L^\infty\left([0,T_\varepsilon];H^m_{\rm per}\right)} \lesssim 1, \quad \|\partial_t\psi(x,t)\|_{L^\infty\left([0,T_\varepsilon];H^{m-2}_{\rm per}\right)} \lesssim 1, \quad m \geq 5.$$

Similar to Theorem 2.7 in the linear case, we shall impose the following non-resonance conditions on the step size τ for TSFP (3.3) in the nonlinear case. For the Fourier modes $|l| \leq \lceil \frac{1}{\tau_0} \rceil$ ($\tau_0 \in (0,1)$), we impose the condition: there exists a constant $C_0 > 0$ such that

$$\left|1 - e^{i\tau\mu_1^2 K}\right| \geq \frac{C_0\tau^{\nu_1}}{(\mu_1^2|K|)^{\nu_2}}, \quad 0 < |K| \leq K_1 = 2\lceil 1/\tau_0\rceil^2, \quad K \in \mathbb{Z}, \tag{3.4}$$

where $\nu_1 \in [0,1]$, $\nu_2 \geq -1$, and the bound $|K| \leq 2\lceil 1/\tau_0\rceil^2$ corresponds to the cubic nonlinear interaction. In particular, we consider the following cases of time step sizes: for a given constant $\alpha \in (0,1)$, the time step size τ satisfies

$$\tau \in \left(0, \alpha\frac{\pi}{\mu_1^2(1+\tau_0)^2}\tau_0^2\right), \tag{3.5}$$

or

$$\tau \in \left\{\tau > 0 : \left|\tau - \frac{2l\pi}{\mu_1^2 K}\right| \geq \frac{\lambda}{|\mu_1^2 K|^{2+\nu_3}}, K, l \in \mathbb{Z},\ 0 < |K| \leq K_1,\ 0 \leq l\right\}, \tag{3.6}$$

where λ and ν_3 are the same as those in (2.28).

Then we have the following improved uniform error bound of the TSFP (3.3) for the NLSE with $O(\varepsilon^2)$-nonlinearity strength up to the time at $O(1/\varepsilon^2)$.

Theorem 3.1. *Let ψ^n be the numerical approximation obtained from the TSFP (3.3). Under the assumption (D), there exist $h_0 > 0$, $0 < \tau_0 < 1$ sufficiently small and independent of ε such that, for any $0 < \varepsilon \leq 1$, when $0 < h < h_0$ and τ satisfies (3.5) or (3.6) ($m \geq 5 + \nu_3$ for (3.6)) with $0 < \tau \leq \tau_1/\varepsilon$ ($\tau_1 > 0$ small enough independent of ε) the following error bounds hold*

$$\begin{aligned} &\|\psi(x,t_n) - I_N\psi^n\|_{H^1} \lesssim h^{m-1} + \varepsilon^2\tau^2 + \tau_0^{m-1}, \\ &\|I_N\psi^n\|_{H^1} \leq 1 + M, \ 0 \leq n \leq \frac{T/\varepsilon^2}{\tau}, \end{aligned} \tag{3.7}$$

where $M := \|\psi\|_{L^\infty([0,T_\varepsilon];H^1)}$. *In particular, if the exact solution is smooth, i.e.* $\psi(x,t) \in H^\infty_{\rm per}$, *the* τ_0^{m-1} *error part would decrease exponentially and can be ignored in practical computation when* τ_0 *is small but fixed, and thus the estimate would practically become*

$$\|\psi(x,t_n) - I_N\psi^n\|_{H^1} \lesssim h^{m-1} + \varepsilon^2\tau^2. \tag{3.8}$$

Remark 3.2. Analogous to the linear case, improved error bounds (3.7) in Theorem 3.1 can be easily generalized to the non-resonance step size (3.4) under slightly different regularity assumptions. We also need $\tau \le \tau_1/\varepsilon$ for controlling the nonlinearity.

Some parts of the proof proceed in analogous lines as the linear case and we omit the details in this section for brevity. Similar to the analysis of the local truncation error for the linear case, we have the following results for the local truncation error for the TSFP (3.3).

Lemma 3.3. *The local truncation error of the TSFP method* (3.3) *for the NLSE with* $O(\varepsilon^2)$*-nonlinearity strength can be written as* $(0 \le n \le \frac{T/\varepsilon^2}{\tau} - 1)$

$$\overline{\mathcal{E}}^n := P_N\mathcal{S}_\tau(P_N\psi(t_n)) - P_N\psi(t_{n+1}) = P_N\mathcal{J}(P_N\psi(t_n)) + Y_n, \tag{3.9}$$

where

$$\mathcal{J}(P_N\psi(t_n)) = -i\varepsilon^2\tau g\left(\frac{\tau}{2}\right) + i\varepsilon^2\int_0^\tau g(s)ds, \tag{3.10}$$

with

$$g(s) = \pm e^{i(\tau-s)\Delta}|P_N(\psi(t_n+s))|^2 e^{is\Delta}P_N\psi(t_n). \tag{3.11}$$

Under the assumption (C), *for* $0 < \varepsilon \le 1$, *we have the error bounds*

$$\|\mathcal{J}(P_N\psi(t_n))\|_{H^1} \lesssim \varepsilon^2\tau^3\|\psi(t_n)\|^3_{H^5}, \quad \|Y_n\|_{H^1} \lesssim \varepsilon^4\tau^3 + \varepsilon^2\tau h^{m-1}. \tag{3.12}$$

Proof for Theorem 3.1. We apply a standard induction argument for proving (3.7). Since $\psi_j^0 = \psi_0(x_j)$, it is obvious for $n = 0$. Assuming the error bounds (3.7) hold true for all $0 \le n \le q \le \frac{T/\varepsilon^2}{\tau} - 1$, we are going to prove the case $n = q+1$. By Fourier projections $\|\psi(x,t_n) - I_N\psi^n\|_{H^1} \lesssim \|P_N\psi(x,t_n) - I_N\psi^n\|_{H^1} + h^{m-1}$, we just need to analyze the growth of the error $e^n = I_N\psi^n - P_N\psi(t_n)$ carefully. For $0 \le n \le q$, we have

$$e^{n+1} = I_N\psi^{n+1} - \mathcal{S}_\tau(P_N\psi(t_n)) + \overline{\mathcal{E}}^n = e^{i\tau\Delta}e^n + Z^n(x) + \overline{\mathcal{E}}^n, \tag{3.13}$$

where $Z^n(x)$ is given by

$$\begin{aligned} Z^n(x) =& e^{i\frac{\tau}{2}\Delta}\Big[I_N((e^{-i\varepsilon^2\tau\lambda|e^{i\frac{\tau}{2}\Delta}I_N\psi^n|^2} - 1)e^{i\frac{\tau}{2}\Delta}I_N\psi^n) \\ & - P_N((e^{-i\varepsilon^2\tau\lambda|e^{i\frac{\tau}{2}\Delta}P_N\psi(t_n)|^2} - 1)e^{i\frac{\tau}{2}\Delta}P_N\psi(t_n))\Big], \end{aligned}$$

with the bound (constant in front of $\|e^n\|_{H^1}$ depends on M)

$$\|Z^n(x)\|_{H^1} \lesssim \varepsilon^2\tau\left(h^{m-1} + \|e^n\|_{H^1}\right). \tag{3.14}$$

From (3.13), we obtain for $0 \le n \le q$,

$$e^{n+1} = e^{i(n+1)\tau\Delta}e^0 + \sum_{k=0}^{n} e^{i(n-k)\tau\Delta}\left(Z^k(x) + \overline{\mathcal{E}}^k\right). \tag{3.15}$$

Similar to the linear case, we get for $0 \le n \le q$,

$$\begin{aligned}\|e^{n+1}\|_{H^1} \lesssim\ & h^{m-1} + \varepsilon^2\tau^2 + \varepsilon^2\tau\sum_{k=0}^{n}\|e^k\|_{H^1} \\ & + \left\|\sum_{k=0}^{n} e^{i(n-k)\tau\Delta}P_N\mathcal{J}(P_N\psi(t_k))\right\|_{H^1}.\end{aligned} \tag{3.16}$$

Recalling (3.10) and (3.11), we could decompose $\mathcal{J}(\psi(t_n))$ as

$$\mathcal{J}(P_N\psi(t_n)) = \mathcal{J}_1(P_N\psi(t_n)) + \mathcal{J}_2(P_N\psi(t_n)), \tag{3.17}$$

where $\mathcal{J}_\sigma(P_N\psi(t_n)) = -i\varepsilon^2\tau g_\sigma(\tau/2) + i\varepsilon^2\int_0^\tau g_\sigma(s)ds$ for $\sigma = 1, 2$ and $g_\sigma(s) := g_\sigma(s; P_N\psi(t_n))$ $(\sigma = 1, 2)$ are defined as

$$g_1(s) = \pm e^{i(\tau-s)\Delta}|e^{is\Delta}P_N\psi(t_n)|^2 e^{is\Delta}P_N\psi(t_n), \quad g_2(s) = g(s) - g_1(s),$$

with $g(s)$ $(s \in [0, \tau])$ given in (3.11). Under the assumption (C), by the Duhamel's principle, it is easy to verify $\||e^{is\Delta}P_N\psi(t_n)|^2 - |P_N\psi(t_n + s)|^2\|_{L^\infty([0,\tau];H^m)} \lesssim \varepsilon^2\tau$. Following similar analysis for the local truncation error in Section 2, for $0 \le n \le \frac{T/\varepsilon^2}{\tau} - 1$, we could arrive at

$$\|\mathcal{J}_1(P_N\psi(t_n))\|_{H^1} \lesssim \varepsilon^2\tau^3, \quad \|\mathcal{J}_2(P_N\psi(t_n))\|_{H^1} \lesssim \varepsilon^4\tau^3. \tag{3.18}$$

In light of (3.16), we find the major part of the error is from $\mathcal{J}_1(\psi_n)$.

Following the RCO approach in the linear case, we introduce the 'twisted variable' $\phi(x,t) = e^{-it\Delta}\psi(x,t)$, and $\|\partial_t\phi\|_{L^\infty([0,T/\varepsilon^2];H^m)} \lesssim \varepsilon^2$ with

$$\|\phi(t_n) - \phi(t_{n-1})\|_{H^m} \lesssim \varepsilon^2\tau, \quad 1 \le n \le \frac{T/\varepsilon^2}{\tau}. \tag{3.19}$$

We choose the same cut-off parameter $\tau_0 \in (0, 1)$ and the corresponding Fourier modes $N_0 = 2\lceil 1/\tau_0\rceil$ as in the proof of Theorem 2.7. Thus, we can derive

$$\left\|e^{n+1}\right\|_{H^1} \lesssim h^{m-1} + \tau_0^{m-1} + \varepsilon^2\tau^2 + \varepsilon^2\tau\sum_{k=0}^{n}\left\|e^k\right\|_{H^1} + \|\mathcal{L}^n\|_{H^1}, \tag{3.20}$$

$$\mathcal{L}^n(x) = \sum_{k=0}^{n} e^{-i(k+1)\tau\Delta}P_{N_0}\mathcal{J}_1(e^{it_k\Delta}(P_{N_0}\phi(t_k))). \tag{3.21}$$

For $l \in \mathcal{T}_{N_0}$, we define the index set $\mathcal{I}_l^{N_0}$ associated to l as

$$\mathcal{I}_l^{N_0} = \{(l_1, l_2, l_3) \mid l_1 - l_2 + l_3 = l,\ l_1, l_2, l_3 \in \mathcal{T}_{N_0}\}. \tag{3.22}$$

Then, the expansion below follows

$$e^{-i(k+1)\tau\Delta}g_1(s; e^{it_k\Delta}P_{N_0}\phi(t_k)) = \pm\sum_{l\in\mathcal{T}_{N_0}}\sum_{(l_1,l_2,l_3)\in\mathcal{I}_l^{N_0}}\mathcal{G}_{k,l,l_1,l_2,l_3}(s)e^{i\mu_l(x-a)},$$

where the coefficients $\mathcal{G}_{k,l,l_1,l_2,l_3}(s)$ are functions of s only,

$$\mathcal{G}_{k,l,l_1,l_2,l_3}(s) = e^{i(t_k+s)\delta_{l,l_1,l_2,l_3}}\left(\widehat{\phi}_{l_2}(t_k)\right)^*\widehat{\phi}_{l_1}(t_k)\widehat{\phi}_{l_3}(t_k), \tag{3.23}$$

and $\delta_{l,l_1,l_2,l_3} = \delta_l - \delta_{l_1} + \delta_{l_2} - \delta_{l_3}$ ($\delta_l = \mu_l^2$ as in (3.23)). The remainder term in (3.16) reads

$$\mathcal{L}^n(x) = \pm i\varepsilon^2 \sum_{k=0}^{n} \sum_{l\in\mathcal{T}_{N_0}} \sum_{(l_1,l_2,l_3)\in\mathcal{I}_l^{N_0}} \Lambda_{k,l,l_1,l_2,l_3} e^{i\mu_l(x-a)}, \tag{3.24}$$

where

$$\begin{aligned}\Lambda_{k,l,l_1,l_2,l_3} &= -\tau\mathcal{G}_{k,l,l_1,l_2,l_3}(\tau/2) + \int_0^\tau \mathcal{G}_{k,l,l_1,l_2,l_3}(s)\,ds \\ &= r_{l,l_1,l_2,l_3} e^{it_k\delta_{l,l_1,l_2,l_3}} c_{k,l,l_1,l_2,l_3}, \end{aligned}\tag{3.25}$$

with coefficients c_{k,l,l_1,l_2,l_3} and r_{l,l_1,l_2,l_3} given by

$$c_{k,l,l_1,l_2,l_3} = (\widehat{\phi}_{l_2}(t_k))^* \widehat{\phi}_{l_1}(t_k)\widehat{\phi}_{l_3}(t_k), \tag{3.26}$$

$$\begin{aligned} r_{l,l_1,l_2,l_3} &= -\tau e^{i\tau\delta_{l,l_1,l_2,l_3}/2} + \int_0^\tau e^{is\delta_{l,l_1,l_2,l_3}}\,ds \\ &= O\left(\tau^3(\delta_{l,l_1,l_2,l_3})^2\right). \end{aligned}\tag{3.27}$$

Similar to the linear case, we only need consider the case $\delta_{l,l_1,l_2,l_3} \neq 0$, as $r_{l,l_1,l_2,l_3} = 0$ if $\delta_{l,l_1,l_2,l_3} = 0$. First, for $l \in \mathcal{T}_{N_0}$ and $(l_1,l_2,l_3) \in \mathcal{I}_l^{N_0}$, we have

$$|\delta_{l,l_1,l_2,l_3}| \le 2\delta_{N_0/2} = 2\mu_{N_0/2}^2 \le \frac{8\pi^2(1+\tau_0)^2}{\tau_0^2(b-a)^2} = \frac{2(1+\tau_0)^2\mu_1^2}{\tau_0^2}, \tag{3.28}$$

which implies for the case (3.5) $0 < \tau \le \alpha\frac{\pi\tau_0^2}{\mu_1^2(1+\tau_0)^2}$ with $0 < \tau_0, \alpha < 1$,

$$\frac{\tau}{2}|\delta_{l,l_1,l_2,l_3}| \le \alpha\pi. \tag{3.29}$$

Denoting $S_{n,l,l_1,l_2,l_3} = \sum_{k=0}^{n} e^{it_k\delta_{l,l_1,l_2,l_3}}$ ($n \ge 0$) and using summation-by-parts, we find from (3.25) that

$$\begin{aligned}\sum_{k=0}^{n}\Lambda_{k,l,l_1,l_2,l_3} &= r_{l,l_1,l_2,l_3}\sum_{k=0}^{n-1} S_{k,l,l_1,l_2,l_3}\left(c_{k,l,l_1,l_2,l_3} - c_{k+1,l,l_1,l_2,l_3}\right) \\ &\quad + S_{n,l,l_1,l_2,l_3}\, r_{l,l_1,l_2,l_3}\, c_{n,l,l_1,l_2,l_3}, \end{aligned}\tag{3.30}$$

and

$$\begin{aligned} &c_{k,l,l_1,l_2,l_3} - c_{k+1,l,l_1,l_2,l_3} \\ &= (\widehat{\phi}_{l_2}(t_k))^*(\widehat{\phi}_{l_1}(t_k) - \widehat{\phi}_{l_1}(t_{k+1}))\widehat{\phi}_{l_3}(t_k) + (\widehat{\phi}_{l_2}(t_k) - \widehat{\phi}_{l_2}(t_{k+1}))^*\widehat{\phi}_{l_1}(t_{k+1})\widehat{\phi}_{l_3}(t_k) \\ &\quad + (\widehat{\phi}_{l_2}(t_{k+1}))^*\widehat{\phi}_{l_1}(t_{k+1})(\widehat{\phi}_{l_3}(t_k) - \widehat{\phi}_{l_3}(t_{k+1})), \end{aligned}\tag{3.31}$$

where c^* is the complex conjugate of c. For the step size in (3.5), we know from (3.29) that for $C = \frac{2\alpha}{\sin(\alpha\pi)}$,

$$|S_{n,l,l_1,l_2,l_3}| \le \frac{1}{|\sin(\tau\delta_{l,l_1,l_2,l_3}/2)|} \le \frac{C}{\tau|\delta_{l,l_1,l_2,l_3}|}, \quad \forall n \ge 0. \tag{3.32}$$

Combining (3.27), (3.30), (3.31) and (3.32), we have

$$\begin{aligned}\left|\sum_{k=0}^{n}\Lambda_{k,l,l_1,l_2,l_3}\right| \lesssim \tau^2|\delta_{l,l_1,l_2,l_3}|\sum_{k=0}^{n-1}\Big(&\left|\widehat{\phi}_{l_1}(t_k)-\widehat{\phi}_{l_1}(t_{k+1})\right|\left|\widehat{\phi}_{l_2}(t_k)\right|\left|\widehat{\phi}_{l_3}(t_k)\right| \\ &+\left|\widehat{\phi}_{l_1}(t_{k+1})\right|\left|\widehat{\phi}_{l_2}(t_k)-\widehat{\phi}_{l_2}(t_{k+1})\right|\left|\widehat{\phi}_{l_3}(t_k)\right| \\ &+\left|\widehat{\phi}_{l_1}(t_{k+1})\right|\left|\widehat{\phi}_{l_2}(t_{k+1})\right|\left|\widehat{\phi}_{l_3}(t_k)-\widehat{\phi}_{l_3}(t_{k+1})\right|\Big) \\ &+\tau^2|\delta_{l,l_1,l_2,l_3}|\left|\widehat{\phi}_{l_1}(t_n)\right|\left|\widehat{\phi}_{l_2}(t_n)\right|\left|\widehat{\phi}_{l_3}(t_n)\right|. \end{aligned} \tag{3.33}$$

Following the discussions in the proof of Theorem 2.7, for the non-resonance step size in (3.6), the same bound in (3.33) holds by replacing $|\delta_{l,l_1,l_2,l_3}|$ with $|\delta_{l,l_1,l_2,l_3}|^{2+\nu_3}$. The rest arguments are almost the same as those for the (3.5) case and we shall only treat the step size (3.5) below.

For $l\in\mathcal{T}_{N_0}$ and $(l_1,l_2,l_3)\in\mathcal{I}_l^{N_0}$, there holds

$$(1+|\mu_l|)|\delta_{l,l_1,l_2,l_3}| \le (1+|\mu_l|)\Big[(\sum_{j=1}^{3}\mu_{l_j})^2+\sum_{j=1}^{3}\mu_{l_j}^2\Big] \lesssim \prod_{j=1}^{3}(1+\mu_{l_j}^2)^{3/2}. \tag{3.34}$$

Based on (3.24), (3.33) and (3.34), we have from (3.16),

$$\begin{aligned}&\|\mathcal{L}^n\|_{H^1}^2 \\ &= \varepsilon^4\sum_{l\in\mathcal{T}_{N_0}}(1+\mu_l^2)\Big|\sum_{(l_1,l_2,l_3)\in\mathcal{I}_l^{N_0}}\sum_{k=0}^{n}\Lambda_{k,l,l_1,l_2,l_3}\Big|^2 \\ &\lesssim \varepsilon^4\tau^4\Bigg\{\sum_{l\in\mathcal{T}_{N_0}}\Bigg(\sum_{(l_1,l_2,l_3)\in\mathcal{I}_l^{N_0}}\left|\widehat{\phi}_{l_1}(t_n)\right|\left|\widehat{\phi}_{l_2}(t_n)\right|\left|\widehat{\phi}_{l_3}(t_n)\right|\prod_{j=1}^{3}(1+\mu_{l_j}^2)^{\frac{3}{2}}\Bigg)^2 \\ &\quad+n\sum_{k=0}^{n-1}\sum_{l\in\mathcal{T}_{N_0}}\Bigg[\Bigg(\sum_{(l_1,l_2,l_3)\in\mathcal{I}_l^{N_0}}\left|\widehat{\phi}_{l_1}(t_k)-\widehat{\phi}_{l_1}(t_{k+1})\right|\left|\widehat{\phi}_{l_2}(t_k)\right|\left|\widehat{\phi}_{l_3}(t_k)\right|\prod_{j=1}^{3}(1+\mu_{l_j}^2)^{\frac{3}{2}}\Bigg)^2 \\ &\quad+\Bigg(\sum_{(l_1,l_2,l_3)\in\mathcal{I}_l^{N_0}}\left|\widehat{\phi}_{l_1}(t_{k+1})\right|\left|\widehat{\phi}_{l_2}(t_k)-\widehat{\phi}_{l_2}(t_{k+1})\right|\left|\widehat{\phi}_{l_3}(t_k)\right|\prod_{j=1}^{3}(1+\mu_{l_j}^2)^{\frac{3}{2}}\Bigg)^2 \\ &\quad+\Bigg(\sum_{(l_1,l_2,l_3)\in\mathcal{I}_l^{N_0}}\left|\widehat{\phi}_{l_1}(t_{k+1})\right|\left|\widehat{\phi}_{l_2}(t_{k+1})\right|\left|\widehat{\phi}_{l_3}(t_k)-\widehat{\phi}_{l_3}(t_{k+1})\right|\prod_{j=1}^{3}(1+\mu_{l_j}^2)^{\frac{3}{2}}\Bigg)^2\Bigg]\Bigg\}. \end{aligned} \tag{3.35}$$

Introducing the auxiliary function $\xi(x)=\sum_{l\in\mathbb{Z}}(1+\mu_l^2)^{\frac{3}{2}}\left|\widehat{\phi}_l(t_n)\right|e^{i\mu_l(x-a)}$, where $\xi(x)\in H_{\rm per}^{m-3}(\Omega)$ implied by assumption (C) and $\|\xi\|_{H^s}\lesssim\|\psi(t_n)\|_{H^{s+3}}$. Expanding $|\xi(x)|^2\xi(x)=\sum_{l\in\mathbb{Z}}\sum_{l_1-l_2+l_3=l}\prod_{j=1}^{3}\left((1+\mu_{l_j}^2)^{\frac{3}{2}}\left|\widehat{\phi}_{l_j}(t_n)\right|\right)e^{i\mu_l(x-a)}$, we could obtain

that

$$\sum_{l\in\mathcal{T}_{N_0}}\Bigg(\sum_{(l_1,l_2,l_3)\in\mathcal{I}_l^{N_0}}\left|\widehat{\phi}_{l_1}(t_n)\right|\left|\widehat{\phi}_{l_2}(t_n)\right|\left|\widehat{\phi}_{l_3}(t_n)\right|\prod_{j=1}^{3}(1+\mu_{l_j}^2)^{\frac{3}{2}}\Bigg)^2$$

$$\le \big\||\xi(x)|^2\xi(x)\big\|_{L^2}^2 \lesssim \|\xi(x)\|_{H^1}^6 \lesssim \|\psi(t_k)\|_{H^4}^6 \lesssim 1. \tag{3.36}$$

Noticing (3.19), we can estimate each terms in (3.35) accordingly as

$$\begin{aligned}&\left\|\sum_{k=0}^{n} e^{-i(k+1)\tau\Delta}P_{N_0}\mathcal{J}_1(e^{it_k\Delta}(P_{N_0}\phi(t_k)))\right\|_{H^1}^2\\ &\lesssim \varepsilon^4\tau^4\left[\|\phi(t_k)\|_{H^4}^6 + n\sum_{k=0}^{n-1}\|\phi(t_k)-\phi(t_{k+1})\|_{H^4}^2\left(\|\phi(t_k)\|_{H^4}+\|\phi(t_{k+1})\|_{H^4}\right)^4\right]\\ &\lesssim \varepsilon^4\tau^4 + n^2\varepsilon^4\tau^4(\varepsilon^2\tau)^2 \lesssim \varepsilon^4\tau^4, \quad n\le q,\end{aligned} \tag{3.37}$$

and (3.20) implies

$$\|e^{n+1}\|_{H^1} \lesssim h^{m-1} + \tau_0^{m-1} + \varepsilon^2\tau^2 + \varepsilon^2\tau\sum_{k=0}^{n}\|e^k\|_{H^1}, \quad 0\le n\le q. \tag{3.38}$$

Using discrete Gronwall's inequality, we have

$$\|e^{q+1}\|_{H^1} \lesssim h^{m-1} + \varepsilon^2\tau^2 + \tau_0^{m-1}, \quad 0\le q\le \frac{T/\varepsilon^2}{\tau} - 1, \tag{3.39}$$

which implies the first inequality in (3.7) at $n = q+1$. There exist $h_0 > 0$ and $\tau_0 > 0$, when $h \le h_0$, τ satisfies (3.5) or (3.6) with $0 < \tau \le \tau_1/\varepsilon$ (τ_1 sufficiently small), the triangle inequality yields that

$$\left\|I_N\psi^{q+1}\right\|_{H^1} \le \|\psi(x,t_{q+1})\|_{H^1} + \left\|e^{q+1}\right\|_{H^1} \le M+1, \quad 0\le q\le \frac{T/\varepsilon^2}{\tau}-1,$$

which means that the induction process for (3.7) is completed. □

Remark 3.4. The improved uniform error bound for the NLSE in Theorem 3.1 is for the cubic nonlinearity without the external potential. It is straightforward to extend to the NLSE with the general nonlinearity $\varepsilon^{2p}|u|^{2p}u$ ($p\in\mathbb{Z}^+$) and the external potential $\varepsilon^{2p}V(x)$. The long-time dynamics of the NLSE with $O(\varepsilon^{2p})$-nonlinearity and $O(1)$-initial data is equivalent to the NLSE with $O(1)$-nonlinearity and $O(\varepsilon)$-initial data. The amplitude of the potential is also $O(\varepsilon^{2p})$, where the scaling is to be consistent with the life-span of the NLSE. The improved H^1-error bound of the TSFP method for the NLSE with $\varepsilon^{2p}|u|^{2p}u$ nonlinearity up to the time at $O(1/\varepsilon^{2p})$ is $O(h^{m-1}+\varepsilon^{2p}\tau^2+\tau_0^{m-1})$. The discussions on removing the parameter τ_0 in Remark 2.11 could be adapted here and we omit the details for brevity.

3.3. **Numerical results.** In this subsection, we present some numerical examples for the NLSE with $O(\varepsilon^2)$-nonlinearity in 1D and 2D to confirm the improved uniform error bound in H^1-norm.

First, we show the long-time temporal errors of the TSFP (3.3) for the NLSE (3.1) on 1D domain $[0,2\pi]$. The initial data is chosen as

$$\psi_0(x) = 2/(2+\sin^2(x)), \quad x\in[0,2\pi]. \tag{3.40}$$

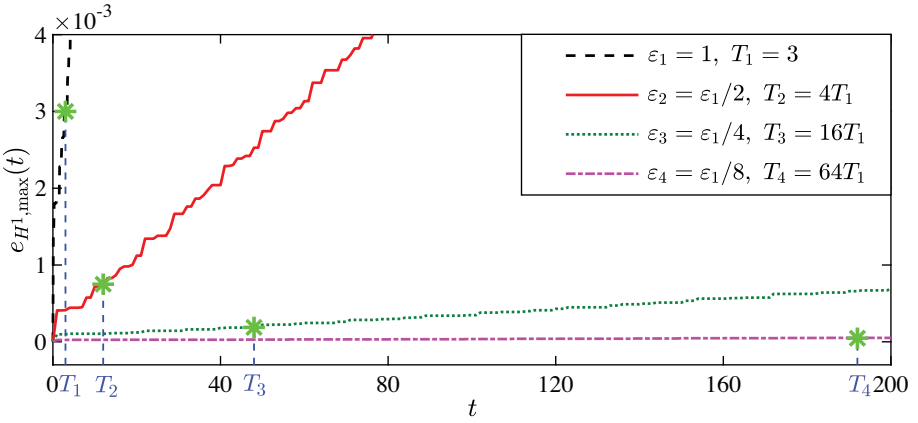

FIGURE 7. Long-time temporal errors in H^1- norm of the TSFP (3.3) for the NLSE (3.1) with different ε

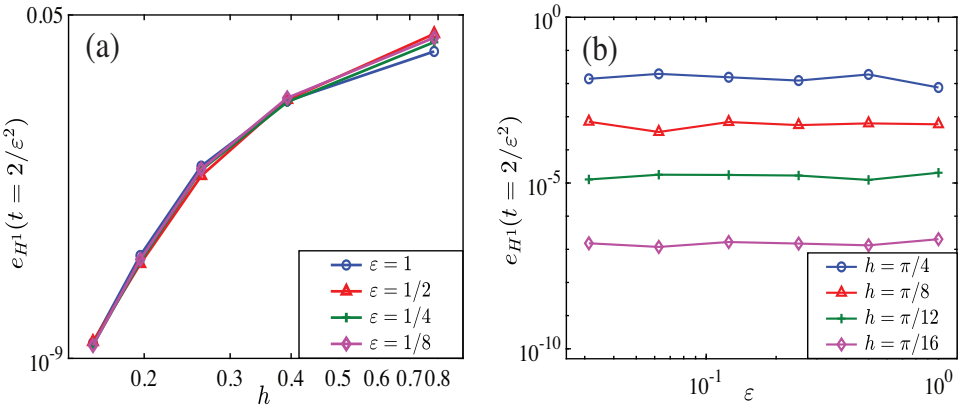

FIGURE 8. Long-time spatial errors in H^1-norm of the TSFP (3.3) for the NLSE in (3.1) at $t = 2/\varepsilon^2$

Figure 7 plots the long-time errors in H^1-norm of the TSFP method for the NLSE with a fixed time step τ and different ε, which indicates that the global errors in H^1-norm behave like $O(\varepsilon^2\tau^2)$ up to the $O(1/\varepsilon^2)$ time. Then, we show the spatial and temporal errors of the TSFP (3.3) for the NLSE (3.1). Figures 8 and 9 depict the long-time spatial and temporal errors of the TSFP (3.3) for the NLSE (3.1) at $t = 2/\varepsilon^2$, respectively. Similar to the linear case, Figure 8 shows the spectral accuracy of the TSFP method for the NLSE in space and the spatial errors are independent of the small parameter ε. Each line in Figure 9 (a) corresponds to a fixed ε and shows the global errors in H^1-norm versus the time step τ, which confirms the second-order convergence of the TSFP method in time. Figure 9 (b) again validates that the global errors in H^1-norm behave like $O(\varepsilon^2\tau^2)$ up to the $O(1/\varepsilon^2)$ time.

Figure 10 displays the long-time errors of the TSFP method for the NLSE (3.1) with large time step size. Each line in Figure 10 (a) plots the long-time errors with

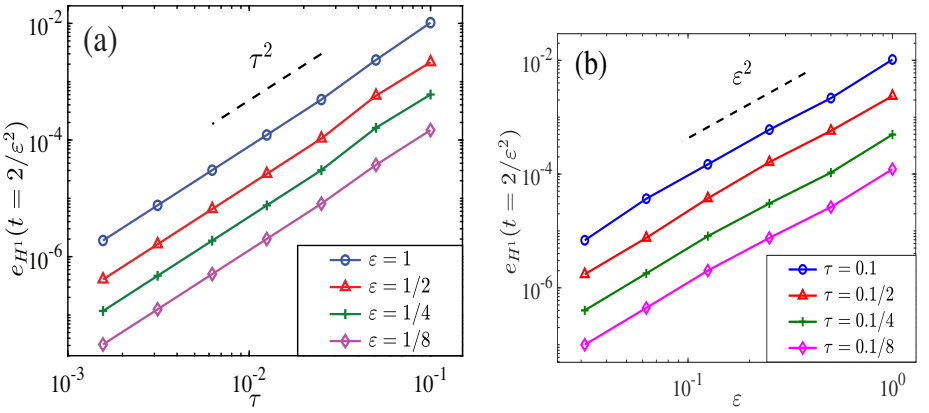

FIGURE 9. Long-time temporal errors in H^1-norm of the TSFP (3.3) for the NLSE (3.1) at $t = 2/\varepsilon^2$

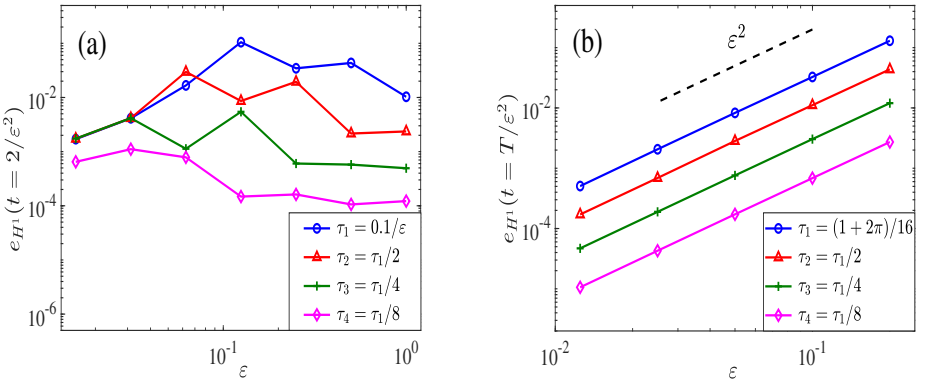

FIGURE 10. Long-time temporal errors in H^1-norm of the TSFP (2.9) for the NLSE (3.1) with large time step size

$\tau = O(1/\varepsilon)$, which are almost constants for different ε, confirming the error bounds. In Figure 10 (b), we choose the larger time step size satisfying the non-resonance condition, which demonstrates the improved uniform error bounds with large time step size.

Then, we show an example in 2D with the irrational aspect ratio of the domain. We choose the domain $\Omega = (0, \pi) \times (0, 1)$ and the initial data

$$\psi_0(x, y) = \frac{1}{1 + \sin^2(2x)} + \sin(2\pi y), \quad \mathbf{x} = (x, y) \in [0, \pi] \times [0, 1]. \tag{3.41}$$

Figure 11 plots the long-time temporal errors in H^1-norm of the TSFP method for the NLSE in 2D with a fixed time step τ and different ε, which confirms that the improved uniform error bound in H^1-norm at $O(\varepsilon^2\tau^2)$ up to the $O(1/\varepsilon^2)$ time is also suitable for the irrational aspect ratio of the domain. Figure 12 depicts the long-time errors for the TSFP method for the NLSE in 2D at $t = 1/\varepsilon^2$, which again

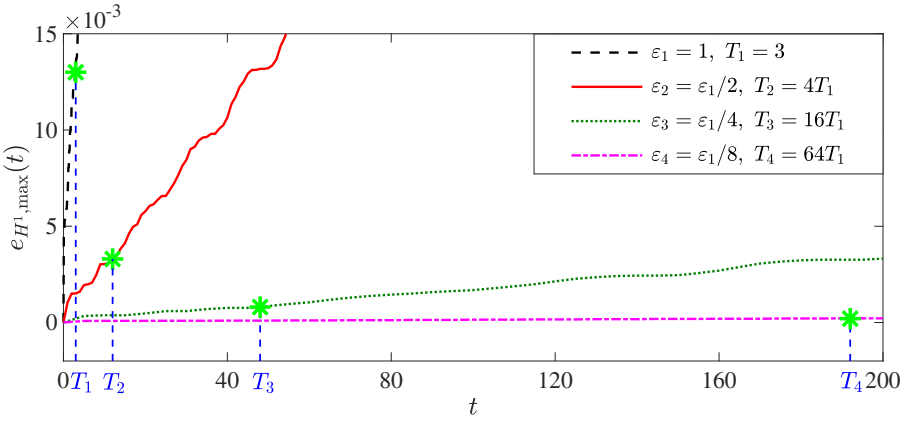

FIGURE 11. Long-time temporal errors in H^1-norm of the TSFP method for the NLSE (1.2) in 2D with different ε

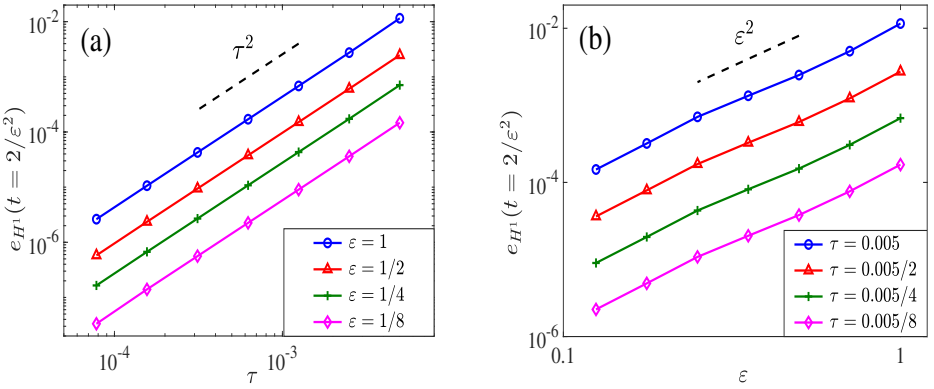

FIGURE 12. Long-time temporal errors in H^1-norm of the TSFP method for the NLSE (1.2) in 2D at $t = 1/\varepsilon^2$

indicates that the TSFP method is second-order in time and validates the improved uniform error bound in H^1-norm up to the time at $O(1/\varepsilon^2)$.

4. Conclusions

Improved uniform error bounds for the time-splitting Fourier pseudospectral (TSFP) methods for the long-time dynamics of the Schrödinger equation with small potential and the nonlinear Schrödinger equation (NLSE) with weak nonlinearity were rigorously established. For the Schrödinger equation with small potential, the linear growth of the uniform error bound in L^2-norm for the TSFP method was strictly proven with the aid of the unitary property of the solution flow in $L^2(\Omega)$. By introducing a new technique of regularity compensation oscillation (RCO), the improved uniform error bound in H^1-norm was carried out at $O(h^{m-1} + \varepsilon\tau^2)$ up to the $O(1/\varepsilon)$ time. In addition, the RCO technique was extended to show the improved uniform error bound $O(h^{m-1} + \varepsilon^2\tau^2)$ for the TSFP method applied to

the cubic NLSE with $O(\varepsilon^2)$-nonlinearity up to the $O(1/\varepsilon^2)$ time. Numerical results were presented to validate our error estimates and demonstrate that they are sharp. We remark here that the RCO technique has been adapted to establish improved uniform error bounds on time-splitting methods for the long-time dynamics of dispersive PDEs including the nonlinear Klein-Gordon equation [5] and the (nonlinear) Dirac equation [6, 9].

Acknowledgment

The authors would like to thank the anonymous referee for the invaluable comments and suggestions.

References

[1] G. D. Akrivis, *Finite difference discretization of the cubic Schrödinger equation*, IMA J. Numer. Anal. **13** (1993), no. 1, 115–124, DOI 10.1093/imanum/13.1.115. MR1199033

[2] X. Antoine, W. Bao, and C. Besse, *Computational methods for the dynamics of the nonlinear Schrödinger/Gross-Pitaevskii equations*, Comput. Phys. Commun. **184** (2013), no. 12, 2621–2633, DOI 10.1016/j.cpc.2013.07.012. MR3128901

[3] W. Bao and Y. Cai, *Mathematical theory and numerical methods for Bose-Einstein condensation*, Kinet. Relat. Models **6** (2013), no. 1, 1–135, DOI 10.3934/krm.2013.6.1. MR3005624

[4] W. Bao and Y. Cai, *Uniform and optimal error estimates of an exponential wave integrator sine pseudospectral method for the nonlinear Schrödinger equation with wave operator*, SIAM J. Numer. Anal. **52** (2014), no. 3, 1103–1127, DOI 10.1137/120866890. MR3199421

[5] W. Bao, Y. Cai, and Y. Feng, *Improved uniform error bounds on time-splitting methods for long-time dynamics of the nonlinear Klein-Gordon equation with weak nonlinearity*, SIAM J. Numer. Anal. **60** (2022), no. 4, 1962–1984, DOI 10.1137/21M1449774. MR4458900

[6] W. Bao, Y. Cai, and Y. Feng, *Improved uniform error bounds on time-splitting methods for the long-time dynamics of the weakly nonlinear Dirac equation*, `arXiv:2203.05886`.

[7] W. Bao, Y. Cai, and J. Yin, *Super-resolution of time-splitting methods for the Dirac equation in the nonrelativistic regime*, Math. Comp. **89** (2020), no. 325, 2141–2173, DOI 10.1090/mcom/3536. MR4109563

[8] W. Bao, Y. Cai, and J. Yin, *Uniform error bounds of time-splitting methods for the nonlinear Dirac equation in the nonrelativistic regime without magnetic potential*, SIAM J. Numer. Anal. **59** (2021), no. 2, 1040–1066, DOI 10.1137/19M1271828. MR4244541

[9] W. Bao, Y. Feng, and J. Yin, *Improved Uniform Error Bounds on Time-Splitting Methods for the Long-Time Dynamics of the Dirac Equation with Small Potentials*, Multiscale Model. Simul. **20** (2022), no. 3, 1040–1062, DOI 10.1137/22M146995X. MR4490286

[10] W. Bao, D. Jaksch, and P. A. Markowich, *Numerical solution of the Gross-Pitaevskii equation for Bose-Einstein condensation*, J. Comput. Phys. **187** (2003), no. 1, 318–342, DOI 10.1016/S0021-9991(03)00102-5. MR1977789

[11] W. Bao, S. Jin, and P. A. Markowich, *On time-splitting spectral approximations for the Schrödinger equation in the semiclassical regime*, J. Comput. Phys. **175** (2002), no. 2, 487–524, DOI 10.1006/jcph.2001.6956. MR1880116

[12] W. Bao and J. Shen, *A fourth-order time-splitting Laguerre-Hermite pseudospectral method for Bose-Einstein condensates*, SIAM J. Sci. Comput. **26** (2005), no. 6, 2010–2028, DOI 10.1137/030601211. MR2196586

[13] C. Besse, B. Bidégaray, and S. Descombes, *Order estimates in time of splitting methods for the nonlinear Schrödinger equation*, SIAM J. Numer. Anal. **40** (2002), no. 1, 26–40, DOI 10.1137/S0036142900381497. MR1921908

[14] J. Bourgain, *Fourier transform restriction phenomena for certain lattice subsets and applications to nonlinear evolution equations. I. Schrödinger equations*, Geom. Funct. Anal. **3** (1993), no. 2, 107–156, DOI 10.1007/BF01896020. MR1209299

[15] J. Bourgain, *Growth of Sobolev norms in linear Schrödinger equations with quasi-periodic potential*, Comm. Math. Phys. **204** (1999), no. 1, 207–247, DOI 10.1007/s002200050644. MR1705671

[16] T. Buckmaster, P. Germain, Z. Hani, and J. Shatah, *Effective dynamics of the nonlinear Schrödinger equation on large domains*, Comm. Pure Appl. Math. **71** (2018), no. 7, 1407–1460, DOI 10.1002/cpa.21749. MR3812076

[17] N. Burq, P. Gérard, and N. Tzvetkov, *Strichartz inequalities and the nonlinear Schrödinger equation on compact manifolds*, Amer. J. Math. **126** (2004), no. 3, 569–605. MR2058384

[18] R. Carles, *On Fourier time-splitting methods for nonlinear Schrödinger equations in the semi-classical limit*, SIAM J. Numer. Anal. **51** (2013), no. 6, 3232–3258, DOI 10.1137/120892416. MR3138106

[19] F. Castella, Ph. Chartier, F. Méhats, and A. Murua, *Stroboscopic averaging for the nonlinear Schrödinger equation*, Found. Comput. Math. **15** (2015), no. 2, 519–559, DOI 10.1007/s10208-014-9235-7. MR3320932

[20] T. Cazenave, *Semilinear Schrödinger Equations*, Courant Lecture Notes in Mathematics, vol. 10, New York University, Courant Institute of Mathematical Sciences, New York; American Mathematical Society, Providence, RI, 2003, DOI 10.1090/cln/010. MR2002047

[21] E. Celledoni, D. Cohen, and B. Owren, *Symmetric exponential integrators with an application to the cubic Schrödinger equation*, Found. Comput. Math. **8** (2008), no. 3, 303–317, DOI 10.1007/s10208-007-9016-7. MR2413146

[22] P. Chartier, F. Méhats, M. Thalhammer, and Y. Zhang, *Improved error estimates for splitting methods applied to highly-oscillatory nonlinear Schrödinger equations*, Math. Comp. **85** (2016), no. 302, 2863–2885, DOI 10.1090/mcom/3088. MR3522973

[23] W. Chen, X. Li, and D. Liang, *Energy-conserved splitting FDTD methods for Maxwell's equations*, Numer. Math. **108** (2008), no. 3, 445–485, DOI 10.1007/s00211-007-0123-9. MR2365825

[24] W. Chen, X. Li, and D. Liang, *Energy-conserved splitting finite-difference time-domain methods for Maxwell's equations in three dimensions*, SIAM J. Numer. Anal. **48** (2010), no. 4, 1530–1554, DOI 10.1137/090765857. MR2684346

[25] D. Cohen, E. Hairer, and C. Lubich, *Modulated Fourier expansions of highly oscillatory differential equations*, Found. Comput. Math. **3** (2003), no. 4, 327–345, DOI 10.1007/s10208-002-0062-x. MR2009682

[26] J. Colliander, M. Keel, G. Staffilani, H. Takaoka, and T. Tao, *Almost conservation laws and global rough solutions to a nonlinear Schrödinger equation*, Math. Res. Lett. **9** (2002), no. 5-6, 659–682, DOI 10.4310/MRL.2002.v9.n5.a9. MR1906069

[27] A. Debussche and E. Faou, *Modified energy for split-step methods applied to the linear Schrödinger equation*, SIAM J. Numer. Anal. **47** (2009), no. 5, 3705–3719, DOI 10.1137/080744578. MR2576517

[28] M. Delfour, M. Fortin, and G. Payre, *Finite-difference solutions of a nonlinear Schrödinger equation*, J. Comput. Phys. **44** (1981), no. 2, 277–288, DOI 10.1016/0021-9991(81)90052-8. MR645840

[29] G. Dujardin, *Exponential Runge-Kutta methods for the Schrödinger equation*, Appl. Numer. Math. **59** (2009), no. 8, 1839–1857, DOI 10.1016/j.apnum.2009.02.002. MR2536086

[30] G. Dujardin and E. Faou, *Normal form and long time analysis of splitting schemes for the linear Schrödinger equation with small potential*, Numer. Math. **108** (2007), no. 2, 223–262, DOI 10.1007/s00211-007-0119-5. MR2358004

[31] L. Erdős, B. Schlein, and H.-T. Yau, *Derivation of the cubic non-linear Schrödinger equation from quantum dynamics of many-body systems*, Invent. Math. **167** (2007), no. 3, 515–614, DOI 10.1007/s00222-006-0022-1. MR2276262

[32] E. Faou, *Geometric Numerical Integration and Schrödinger Equations*, Zurich Lectures in Advanced Mathematics, European Mathematical Society (EMS), Zürich, 2012, DOI 10.4171/100. MR2895408

[33] E. Faou, L. Gauckler, and C. Lubich, *Sobolev stability of plane wave solutions to the cubic nonlinear Schrödinger equation on a torus*, Comm. Partial Differential Equations **38** (2013), no. 7, 1123–1140, DOI 10.1080/03605302.2013.785562. MR3169740

[34] E. Faou, P. Germain, and Z. Hani, *The weakly nonlinear large-box limit of the 2D cubic nonlinear Schrödinger equation*, J. Amer. Math. Soc. **29** (2016), no. 4, 915–982, DOI 10.1090/jams/845. MR3522607

[35] E. Faou, B. Grébert, and E. Paturel, *Birkhoff normal form for splitting methods applied to semilinear Hamiltonian PDEs. I. Finite-dimensional discretization*, Numer. Math. **114** (2010), no. 3, 429–458, DOI 10.1007/s00211-009-0258-y. MR2570074

[36] L. Gauckler and C. Lubich, *Nonlinear Schrödinger equations and their spectral semi-discretizations over long times*, Found. Comput. Math. **10** (2010), no. 2, 141–169, DOI 10.1007/s10208-010-9059-z. MR2594442

[37] L. Gauckler and C. Lubich, *Splitting integrators for nonlinear Schrödinger equations over long times*, Found. Comput. Math. **10** (2010), no. 3, 275–302, DOI 10.1007/s10208-010-9063-3. MR2628827

[38] E. Hairer, C. Lubich, and G. Wanner, *Geometric Numerical Integration*, Springer Series in Computational Mathematics, vol. 31, Springer, Heidelberg, 2010. Structure-preserving algorithms for ordinary differential equations; Reprint of the second (2006) edition. MR2840298

[39] S. Herr, D. Tataru, and N. Tzvetkov, *Strichartz estimates for partially periodic solutions to Schrödinger equations in 4d and applications*, J. Reine Angew. Math. **690** (2014), 65–78, DOI 10.1515/crelle-2012-0013. MR3200335

[40] M. Hochbruck and A. Ostermann, *Exponential integrators*, Acta Numer. **19** (2010), 209–286, DOI 10.1017/S0962492910000048. MR2652783

[41] T. Jahnke and C. Lubich, *Error bounds for exponential operator splittings*, BIT **40** (2000), no. 4, 735–744, DOI 10.1023/A:1022396519656. MR1799313

[42] C. Lubich, *On splitting methods for Schrödinger-Poisson and cubic nonlinear Schrödinger equations*, Math. Comp. **77** (2008), no. 264, 2141–2153, DOI 10.1090/S0025-5718-08-02101-7. MR2429878

[43] R. I. McLachlan and G. R. W. Quispel, *Splitting methods*, Acta Numer. **11** (2002), 341–434, DOI 10.1017/S0962492902000053. MR2009376

[44] Z.-j. Shang, *Resonant and Diophantine step sizes in computing invariant tori of Hamiltonian systems*, Nonlinearity **13** (2000), no. 1, 299–308, DOI 10.1088/0951-7715/13/1/314. MR1734634

[45] J. Shen, T. Tang, and L.-L. Wang, *Spectral Methods: Algorithms, Analysis and Applications*, Springer-Verlag Berlin Heidelberg, 2011.

[46] G. Strang, *On the construction and comparison of difference schemes*, SIAM J. Numer. Anal. **5** (1968), 506–517, DOI 10.1137/0705041. MR235754

[47] C. Sulem and P.-L. Sulem, *The Nonlinear Schrödinger Equation*, Applied Mathematical Sciences, vol. 139, Springer-Verlag, New York, 1999. Self-focusing and wave collapse. MR1696311

[48] T. Tao, *Nonlinear Dispersive Equations*, CBMS Regional Conference Series in Mathematics, vol. 106, Published for the Conference Board of the Mathematical Sciences, Washington, DC; by the American Mathematical Society, Providence, RI, 2006. Local and global analysis, DOI 10.1090/cbms/106. MR2233925

[49] M. Thalhammer, *High-order exponential operator splitting methods for time-dependent Schrödinger equations*, SIAM J. Numer. Anal. **46** (2008), no. 4, 2022–2038, DOI 10.1137/060674636. MR2399406

[50] M. Thalhammer, *Convergence analysis of high-order time-splitting pseudospectral methods for nonlinear Schrödinger equations*, SIAM J. Numer. Anal. **50** (2012), no. 6, 3231–3258, DOI 10.1137/120866373. MR3022261

[51] W.-M. Wang, *Bounded Sobolev norms for linear Schrödinger equations under resonant perturbations*, J. Funct. Anal. **254** (2008), no. 11, 2926–2946, DOI 10.1016/j.jfa.2007.11.012. MR2414227

[52] J. A. C. Weideman and B. M. Herbst, *Split-step methods for the solution of the nonlinear Schrödinger equation*, SIAM J. Numer. Anal. **23** (1986), no. 3, 485–507, DOI 10.1137/0723033. MR842641

Department of Mathematics, National University of Singapore, Singapore 119076
Email address: matbaowz@nus.edu.sg

Laboratory of Mathematics and Complex Systems and School of Mathematical Sciences, Beijing Normal University, Beijing 100875, People's Republic of China
Email address: yongyong.cai@bnu.edu.cn

Department of Mathematics, National University of Singapore, Singapore 119076
Email address: fengyue@u.nus.edu